Indiana Michigan
Power Company
500 Circle Drive
Buchanan, MI 49107 1373

INDIANA MICHIGAN POWER

October 15, 2002
AEP:NRC:2900-02
10 CFR 50.90

U. S. Nuclear Regulatory Commission
ATTN: Document Control Desk
Mail Stop O-P1-17
Washington, DC 20555-0001

SUBJECT: Donald C. Cook Nuclear Plant Unit 1
Docket No. 50-315
Supplement to License Amendment Request for Appendix K Measurement Uncertainty Recapture – Power Uprate Request (TAC No. MB5498)

References:

1) Letter from J. E. Pollock, I&M, to Nuclear Regulatory Commission (NRC) Document Control Desk, "License Amendment Request for Appendix K Measurement Uncertainty Recapture – Power Uprate Request," AEP:NRC:2900, dated June 28, 2002

2) Letter from J. F. Stang, NRC, to A. C. Bakken III, I&M, "Donald C. Cook Nuclear Plant, Unit 1 – Request for Additional Information Regarding License Amendment Request, 'Power Uprate Measurement Uncertainty Recapture,' dated June 28, 2002 (TAC Nos. MB5498)," dated October 2, 2002

3) Letter from J. E. Pollock, I&M, to NRC Document Control Desk, "Response to Nuclear Regulatory Commission Request for Additional Information Regarding License Amendment Request for Appendix K Measurement Uncertainty Recapture - Power Uprate Request," AEP:NRC:2900-01, dated October 15, 2002

This letter supplements a previously submitted amendment request for an increase in the Donald C. Cook Nuclear Plant (CNP) Unit 1 licensed reactor core power level.

A001

By Reference 1, Indiana Michigan Power Company (I&M), the licensee for CNP Unit 1, proposed to amend Facility Operating License DPR-58 to increase the maximum reactor core power level permitted by the license. By Reference 2, the NRC requested additional information regarding the amendment proposed in Reference 1. By Reference 3, I&M responded to the request for additional information transmitted by Reference 2. Reference 3 documents I&M's commitment, made in an August 13, 2002, telephone conference, to revise the applicability limit proposed in Reference 1 for the Reactor Coolant System (RCS) pressure-temperature curves contained in the Technical Specifications (TS). Reference 3 also documents I&M's commitment to withdraw the proposed change to the TS that governs the reactor vessel capsule removal intervals. This letter fulfills these two commitments.

Enclosure 1 provides an oath and affirmation affidavit pertaining to the statements made and the matters set forth in this letter. Enclosure 2 provides a detailed description and technical evaluation to support the proposed supplement. Attachment 1 provides new marked-up TS pages to replace the corresponding pages submitted in Attachment 1 to Reference 1. Attachment 2 provides new TS pages, with the changes incorporated, to replace the corresponding pages submitted in Attachment 2 to Reference 1. Attachment 3 provides a summary of the computation that was performed to determine the new applicability limit for the RCS pressure-temperature curves. Attachment 4 provides the fluence analysis used in the applicability limit computation summarized in Attachment 3. Attachment 5 addresses the Unit 1 applicability of NRC questions pertaining to a proposed change to the Unit 2 RCS pressure-temperature curves. Attachment 6 identifies the commitment documented in this letter.

The applicability limit for the RCS pressure-temperature curves proposed in this letter is more restrictive than the applicability limit previously proposed in Reference 1. The withdrawal of the proposed change to the reactor vessel capsule removal schedule documented in this letter represents a reduction in the scope of the change previously proposed in Reference 1. Therefore, the No Significant Hazards Consideration evaluation and the evaluation of Environmental Considerations provided in Enclosure 2 to Reference 1 bound the changes proposed in this letter and remain valid.

Should you have any questions, please contact Mr. Brian A. McIntyre, Manager of Regulatory Affairs, at (269) 697-5806.

Sincerely,

J. E. Pollock
Site Vice President

NH/jen

Enclosures:

1. Oath and Affirmation Affidavit
2. Detailed Description and Technical Evaluation of Proposed Changes

Attachments:

1. Unit 1 Technical Specifications Pages Marked to Show Proposed Changes
2. Proposed Unit 1 Technical Specifications Pages with Changes Incorporated
3. Computation of Revised Applicability Limit for Unit 1 Reactor Coolant System Pressure-Temperature Curves
4. Radiation Analysis and Neutron Dosimetry for the Donald C. Cook Nuclear Plant Unit 1 Measurement Uncertainty Recapture
5. Applicability of NRC Questions Pertaining to Unit 2 Reactor Coolant System Pressure-Temperature Curve Changes
6. Regulatory Commitments

c: K. D. Curry, AEP Ft. Wayne, w/o attachments
J. E. Dyer, NRC Region III
MDEQ - DW & RPD, w/o attachments
NRC Resident Inspector
J. F. Stang, Jr., NRC Washington, DC
R. Whale, MPSC, w/o attachments

bc: G. P. Arent
A. C. Bakken III
M. J. Finissi
S. A. Greenlee
G. J. Hill
D. W. Jenkins, w/o attachments
J. B. Kingseed/R. J. Kohrt
J. A. Kobyra, w/o attachments
B. A. McIntyre, w/o attachments
J. E. Newmiller
J. E. Pollock
K. W. Riches
T. R. Satyan-Sharma
M. K. Scarpello, w/o attachments
T. R. Stephens
T. K. Woods, w/o attachments

AFFIRMATION

I, Joseph E. Pollock, being duly sworn, state that I am Site Vice President of Indiana Michigan Power Company (I&M), that I am authorized to sign and file this request with the Nuclear Regulatory Commission on behalf of I&M, and that the statements made and the matters set forth herein pertaining to I&M are true and correct to the best of my knowledge, information, and belief.

Indiana Michigan Power Company

J. E. Pollock
Site Vice President

SWORN TO AND SUBSCRIBED BEFORE ME

THIS 15 DAY OF October, 2002

Notary Public

My Commission Expires 5/26/05

JENNIFER L KERNOSKY
Notary Public, Berrien County, Michigan
My Commission Expires May 26, 2005

DETAILED DESCRIPTION AND TECHNICAL EVALUATION OF PROPOSED CHANGES

1. DESCRIPTION

By Reference 1, Indiana Michigan Power Company (I&M) proposed to amend the Donald C. Cook Nuclear Plant (CNP) Unit 1 Facility Operating License, including the Technical Specifications (TS), to increase the licensed reactor core power level. By Reference 2, the NRC requested additional information regarding the amendment proposed in Reference 1. By Reference 3, I&M responded to the request for additional information transmitted by Reference 2. Reference 3 documented I&M's commitment to revise the applicability limit proposed in Reference 1 for the Reactor Coolant System (RCS) pressure-temperature curves contained in the TS, and to withdraw the TS change proposed in Reference 1 pertaining to the reactor vessel capsule removal schedule. This letter fulfills these two commitments.

2. PROPOSED CHANGE

I&M proposes the following specific changes to the amendment proposed in Reference 1:

- I&M proposes to revise the two notes on TS Figure 3.4-2, "Reactor Coolant System Pressure-Temperature Limits Versus 60°F/hr Rate Criticality Limit and Hydrostatic Test Limit," and the two notes on TS Figure 3.4-3, "Reactor Coolant System Pressure-Temperature Limits Versus Cooldown Rates," such that the current limit of applicability, 32 effective full power years (EFPY), would be changed to 18.6 EFPY. This proposed applicability limit supercedes the limit of 28.4 EFPY that was proposed by Reference 1.

- I&M withdraws the change proposed in Reference 1 to TS Table 4.4-5, "Reactor Vessel Material Irradiation Surveillance Schedule." That change would have revised the removal interval for Capsule S from "32 EFPY" to "Standby."

- I&M proposes to revise the Bases for TS 3/4.4.9, "Pressure/Temperature Limits," to be consistent with the above-described revisions. This Bases change supercedes the change to the Bases for TS 3/4.4.9 that was proposed by Reference 1.

Attachment 1 to this letter provides new marked-up TS pages to replace the corresponding pages submitted in Attachment 1 to Reference 1. Attachment 2 provides new TS pages, with the changes incorporated, to replace the corresponding pages submitted in Attachment 2 to Reference 1.

3. BACKGROUND

In June 2000, the Nuclear Regulatory Commission (NRC) approved a revision to 10 CFR 50, Appendix K, "ECCS Evaluation Models," allowing licensees to recapture margin used in emergency core cooling system (ECCS) evaluations to account for uncertainties due to power level instrumentation error. Based on implementation of more accurate feedwater flow measurement instrumentation and associated power calorimetric uncertainty values, I&M submitted an amendment request (Reference 1) to increase the Unit 1 licensed core power by 1.66 percent, from 3250 MWt to 3304 MWt. This increase in licensed core power is referred to as the Margin Uncertainty Recapture (MUR) uprate.

In support of the proposed amendment, the MUR uprate was evaluated for impact on the nuclear steam supply system and balance of plant systems, and on the associated safety analyses. This evaluation determined that the increased neutron fluence associated with the MUR uprate would necessitate a change to the applicability limit for the existing RCS pressure-temperature curves in TS Figure 3.4-2 and TS Figure 3.4-3. Based on the reactor vessel integrity evaluation performed for the MUR uprate, I&M proposed changing the applicability limit for the existing curves from 32 EFPY to 28.4 EFPY. The MUR uprate evaluation also determined that the criteria associated with both the fourth and fifth reactor vessel surveillance capsule removal intervals specified in TS Table 4.4-5 were satisfied by the fourth capsule, Capsule U, which had been previously removed. Consequently, I&M proposed to revise TS Table 4.4-5, by changing the removal interval for the fifth capsule, Capsule S, from "32 EFPY" to "Standby."

In a letter dated June 28, 1999 (Reference 4), I&M identified a new limiting reactor vessel beltline material for CNP Unit 1, and committed to submit new heatup and cooldown curves and new low temperature overpressure protection (LTOP) setpoints. In a letter dated May 3, 2002 (Reference 5), I&M stated that, based on the new limiting reactor vessel beltline material, the existing heatup and cooldown curves would remain valid until at least the end of April 2005. In Reference 5, I&M committed to submit new heatup and cooldown curves and new LTOP setpoints no later than April 30, 2004.

In an August 13, 2002, telephone conference with the NRC Staff, I&M committed to revise the 28.4 EFPY applicability limit proposed in Reference 1 to include the effects of the limiting reactor vessel beltline material identified in Reference 4, along with the effects of the increased neutron fluence associated with the MUR uprate. I&M also committed to withdraw the proposed change to the reactor vessel surveillance capsule removal schedule, since implementation of that change is not required for the MUR uprate. By Reference 2, the NRC requested additional information regarding the amendment proposed in Reference 1. Reference 3, which provided I&M's response to Reference 2, documented the commitments made in the August 13, 2002, telephone conference regarding the RCS pressure-temperature curve applicability limit and the reactor vessel surveillance capsule removal schedule.

In the August 13, 2002, telephone conference, I&M also committed to submit, by December 31, 2002, a proposed license amendment containing new Unit 1 RCS

pressure-temperature curves that reflect the limiting reactor vessel beltline material. I&M anticipates that use of new fluence analysis methodology and new American Society of Mechanical Engineers Boiler and Pressure Vessel Code Cases will result in new curves that are less restrictive than the existing curves. I&M does not intend to include new LTOP setpoints in the proposed amendment unless the new pressure-temperature curves are more restrictive than the existing curves. This commitment supercedes I&M's previous commitment, made in Reference 5, to submit new curves and new LTOP setpoints by April 30, 2004.

In a letter dated July 23, 2002 (Reference 6), I&M proposed to revise the Unit 2 RCS pressure-temperature curves. By Reference 7, the NRC requested additional information regarding the amendment proposed by Reference 6. Although the Unit 2 licensing activity proposed by Reference 6 is unrelated to the proposed Unit 1 RCS pressure-temperature curve applicability limit changes, I&M has reviewed the NRC's questions for impact on the changes proposed by this letter. Attachment 5 presents I&M's responses to the NRC's questions, as applied to the proposed Unit 1 pressure-temperature curve applicability limit changes.

4. TECHNICAL ANALYSIS

The technical basis for the new applicability limit of 18.6 EFPY in TS Figure 3.4-2 and TS Figure 3.4-3 is provided by the computation summarized in Attachment 3 to this letter. As stated in Attachment 3, the computation is based on the fluence resulting from the MUR uprate that was determined as described in Attachment 4. The technical basis for the proposed applicability limit provided in Attachment 3 takes into consideration questions posed by the NRC in Reference 7 on the changes I&M proposed in Reference 6 to the Unit 2 RCS pressure-temperature curves. The applicability of these questions to the Unit 1 pressure-temperature curve changes proposed in this letter is addressed in Attachment 5.

5. REGULATORY SAFETY ANALYSIS

No Significant Hazards Consideration

As described in the transmittal letter for this supplement, the No Significant Hazards Consideration evaluation provided in Enclosure 2 to Reference 1 remains valid.

Applicable Regulatory Requirements/Criteria

The discussion of applicable regulatory requirements/criteria provided in Enclosure 2 to Reference 1 remains valid.

6. ENVIRONMENTAL CONSIDERATION

As described in the transmittal letter for this supplement, the evaluation of Environmental Considerations provided in Enclosure 2 to Reference 1 remains valid.

7. REFERENCES

1. Letter from J. E. Pollock, I&M, to NRC Document Control Desk, "License Amendment Request for Appendix K Measurement Uncertainty Recapture – Power Uprate Request," AEP:NRC:2900, dated June 28, 2002
2. Letter from J. F. Stang, NRC, to A. C. Bakken III, I&M, "Donald C. Cook Nuclear Plant, Unit 1 – Request for Additional Information Regarding License Amendment Request, 'Power Uprate Measurement Uncertainty Recapture,' dated June 28, 2002 (TAC No. MB5498)," dated October 2, 2002
3. Letter from J. E. Pollock, I&M, to NRC Document Control Desk, "Response to Nuclear Regulatory Commission Request for Additional Information Regarding License Amendment Request for Appendix K Measurement Uncertainty Recapture - Power Uprate Request," AEP:NRC:2900-01, dated October 15, 2002
4. Letter from M. W. Rencheck, I&M, to NRC Document Control Desk, "Request for Additional Information (RAI) Regarding Reactor Pressure Vessel Integrity at Donald C. Cook Nuclear Plant, Unit 1, TAC No. MA0539," C0699-01, dated June 28, 1999
5. Letter from J. E. Pollock, I&M, to NRC Document Control Desk, "Revised Commitment Date Regarding Generic Letter 92-01, Supplement 1, Reactor Vessel Structural Integrity," AEP:NRC:2349, dated May 3, 2002
6. Letter from J. E. Pollock, I&M, to NRC Document Control Desk, "License Amendment Request for Unit 2 Reactor Coolant System Pressure-Temperature Curves, and Request for Exemption from Requirements in 10 CFR 50.60(a) and 10 CFR 50, Appendix G," AEP:NRC:2349-01, dated July 23, 2002
7. Letter from J. F. Stang, NRC, to A. C. Bakken III, I&M, "Donald C. Cook Nuclear Plant, Unit 2 – Request for Additional Information Regarding License Amendment Request, 'Reactor Coolant System Pressure – Temperature Curves,' dated July 23, 2002," dated September 27, 2002

ATTACHMENT 1 TO AEP:NRC:2900-02

UNIT 1 TECHNICAL SPECIFICATIONS PAGES
MARKED TO SHOW PROPOSED CHANGES

REVISED PAGES

3/4 4-27
3/4 4-28
B 3/4 4-6
B 3/4 4-7

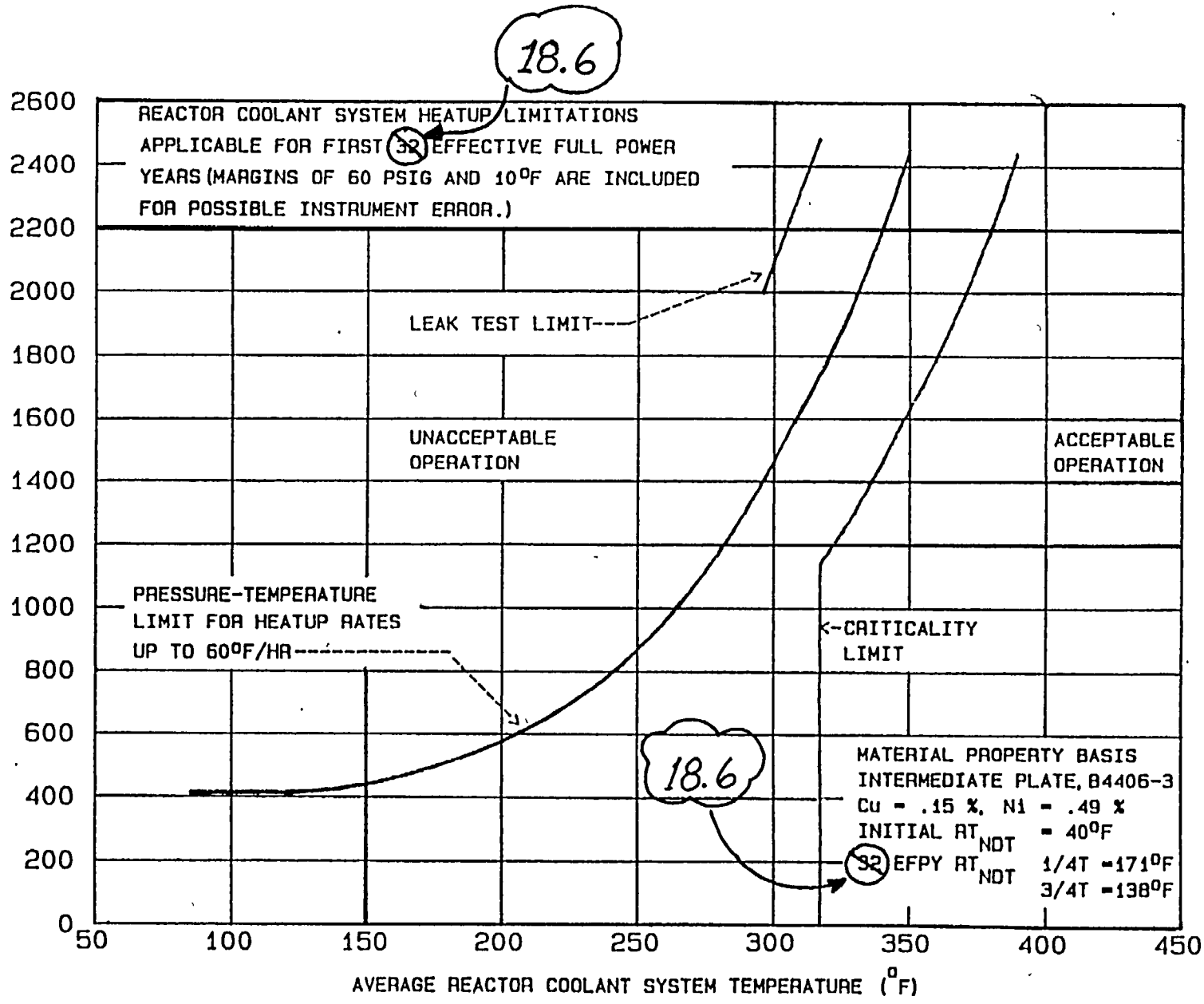

FIGURE 3.4-2

REACTOR COOLANT SYSTEM PRESSURE - TEMPERATURE LIMITS VERSUS 60° F/HR RATE
CRITICALITY LIMIT AND HYDROSTATIC TEST LIMIT

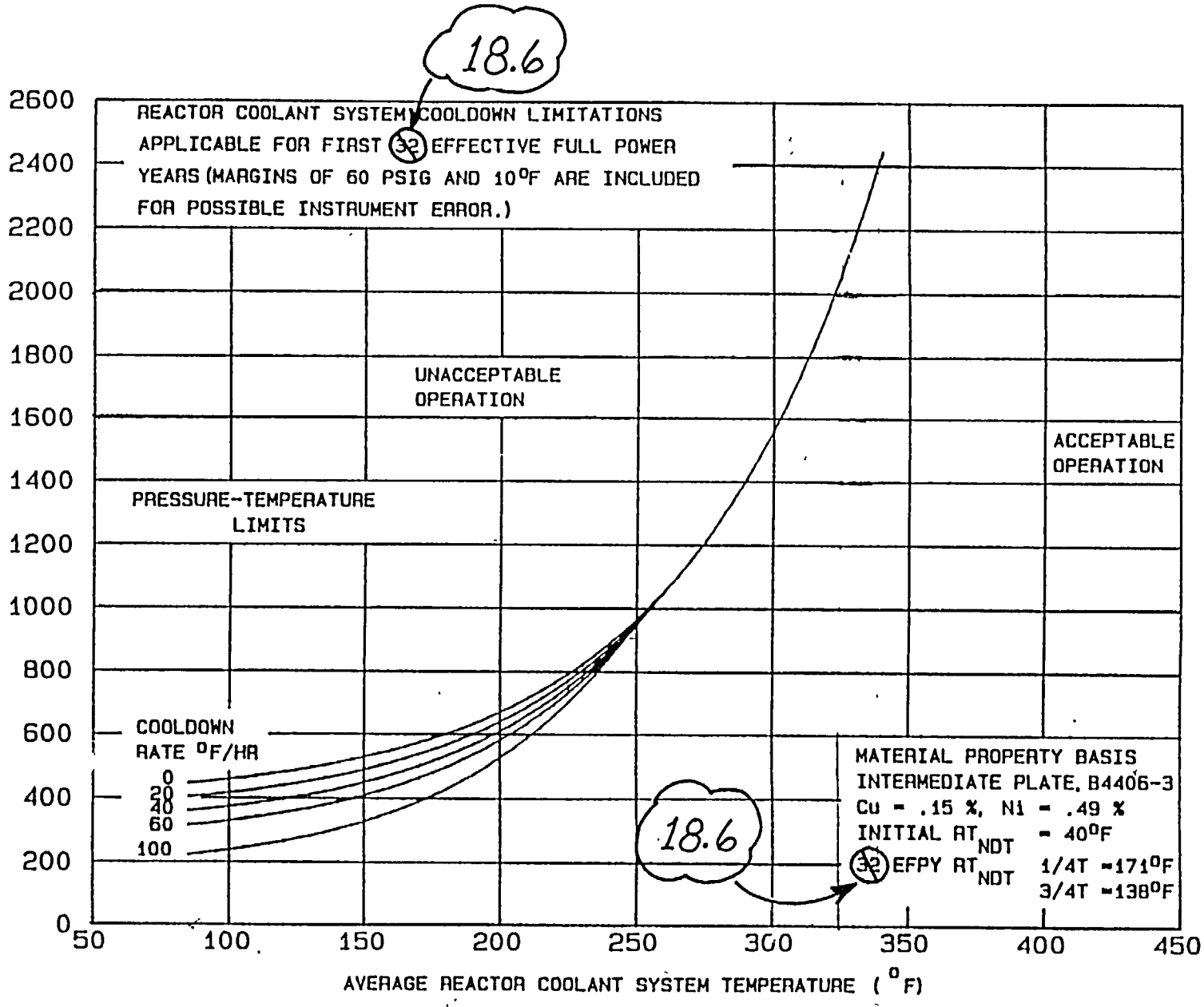

FIGURE 3.4-3

REACTOR COOLANT SYSTEM PRESSURE - TEMPERATURE LIMITS VERSUS COOLDOWN RATES

3/4.4.9 PRESSURE/TEMPERATURE LIMITS

All components in the Reactor Coolant system are designed to withstand the effects of cyclic loads due to system temperature and pressure changes. These cyclic loads are introduced by normal load transients, reactor trips, and startup and shutdown operations. The various categories of load cycles used for design purposes are provided in Section 4.1.4 of the FSAR. During startup and shutdown, the rates of temperature and pressure changes are limited so that the maximum specified heatup and cooldown rates are consistent with the design assumptions and satisfy the stress limits for cyclic operation.

An ID or OD one-quarter thickness surface flaw is postulated at the location in the vessel which is found to be the limiting case. There are several factors which influence the postulated location. The thermal induced bending stress during heatup is compressive on the inner surface while tensile on the outer surface of the vessel wall. During cooldown the bending stress profile is reversed. In addition, the material toughness is dependent upon irradiation and temperature and therefore the fluence profile through the reactor vessel wall, the rate of heatup and also the rate of cooldown influence the postulated flaw location.

The heatup limit curve, Figure 3.4-2, is a composite curve which was prepared by determining the most conservative case, with either the inside or outside wall controlling, for any heatup rate up to 60°F per hour. The cooldown limit curves of Figure 3.4-3 are composite curves which were prepared based upon the same type analysis with the exception that the controlling location is always the inside wall where the cooldown thermal gradients tend to produce tensile stresses while producing compressive stresses at the outside wall. The heatup and cooldown curves were prepared based upon the most limiting value of the predicted adjusted reference temperature at the end of ~~32~~ 18.6 EFPY.

Reactor operation and resultant fast neutron (E > 1 Mev) irradiation will cause an increase in the RT_{NDT}. Therefore, an adjusted reference temperature, based upon the fluence, and the copper and nickel content of the material must be predicted. The heatup and cooldown limit curves of Figures 3.4-2 and 3.4-3 include the adjusted RT_{NDT} at the end of ~~32~~ 18.6 EFPY, as well as adjustments for possible errors in the pressure and temperature sensing instruments.

The ~~32~~ 18.6 EFPY heatup and cooldown curves were developed based on the following:

1. The intermediate shell plate, B4406-3, being the limiting material with a copper and nickel content of .15% and .49%, respectively.

2. The fluence values ~~contained in Table 6-14 of Westinghouse's WCAP-12483 report, "Analysis of Capsule U From the American Electric Power Company D.C. Cook Unit 1 Reactor Vessel Radiation Surveillance Program," dated January 1990~~ documented in I&M letter AEP:NRC:2900-02.

3. Figure 1, NRC Regulatory Guide 1.99, Revision 2

The shift in RT_{NDT} of the reactor vessel material has been established by removing and evaluating the material surveillance capsules installed near the inside wall of the reactor vessel in accordance with the removal schedule in Table 4.4-5. Per this schedule, Capsule U is the last capsule to be removed until Capsule S is to be removed after 32 EFPY (EOL). Capsule V, W, and Z will remain in the reactor vessel, and will be removed to address industry reactor embrittlement concerns, if required.

The pressure-temperature limit lines shown on Figure 3.4-2 for reactor criticality and for inservice leak and hydrostatic testing have been provided to assure compliance with the minimum temperature requirements of Appendix G to 10 CFR 50.

The number of reactor vessel irradiation surveillance specimens and the frequencies for removing these specimens are provided in Table 4.4-5 to assure compliance with the requirements of Appendix H to 10 CFR Part 50

The limitations imposed on pressurizer heatup and cooldown and spray water temperature differential are provided to assure that the pressurizer is operated within the design criteria assumed for the fatigue analysis performed in accordance with the ASME Code requirements.

The OPERABILITY of two PORVs, or of one PORV and the RHR safety valve, ensures that the RCS will be protected from pressure transients which could exceed the limits of Appendix G to 10 CFR Part 50 when one or more of the RCS cold legs are less than or equal to 152°F. Either PORV or RHR safety valve has adequate relieving capability to protect the RCS from overpressurization when the transient is limited to either (1) the start of an idle RCP with the secondary water temperature of the steam generator less than or equal to 50°F above the RCS cold leg temperatures or (2) the start of a charging pump and its injection into a water solid RCS. Therefore, any one of the three blocked open PORVs constituted an acceptable RCS vent to preclude APPLICABILITY of Specification 3.4.9.3.

ATTACHMENT 2 TO AEP:NRC:2900-02

PROPOSED UNIT 1 TECHNICAL SPECIFICATIONS PAGES WITH CHANGES INCORPORATED

REVISED PAGES

3/4 4-27
3/4 4-28
B 3/4 4-6
B 3/4 4-7

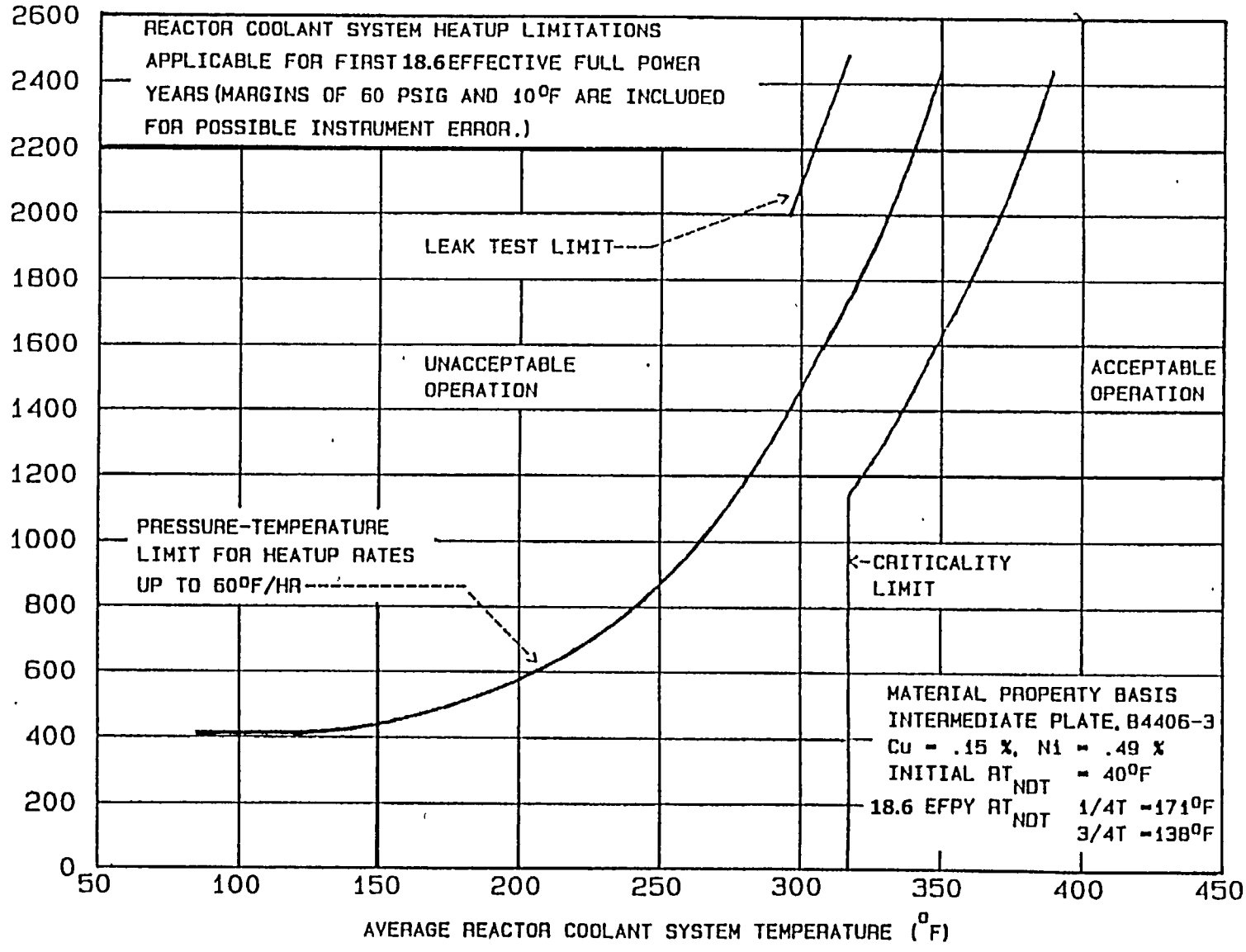

FIGURE 3.4-2

REACTOR COOLANT SYSTEM PRESSURE - TEMPERATURE LIMITS VERSUS 60° F/HR RATE
CRITICALITY LIMIT AND HYDROSTATIC TEST LIMIT

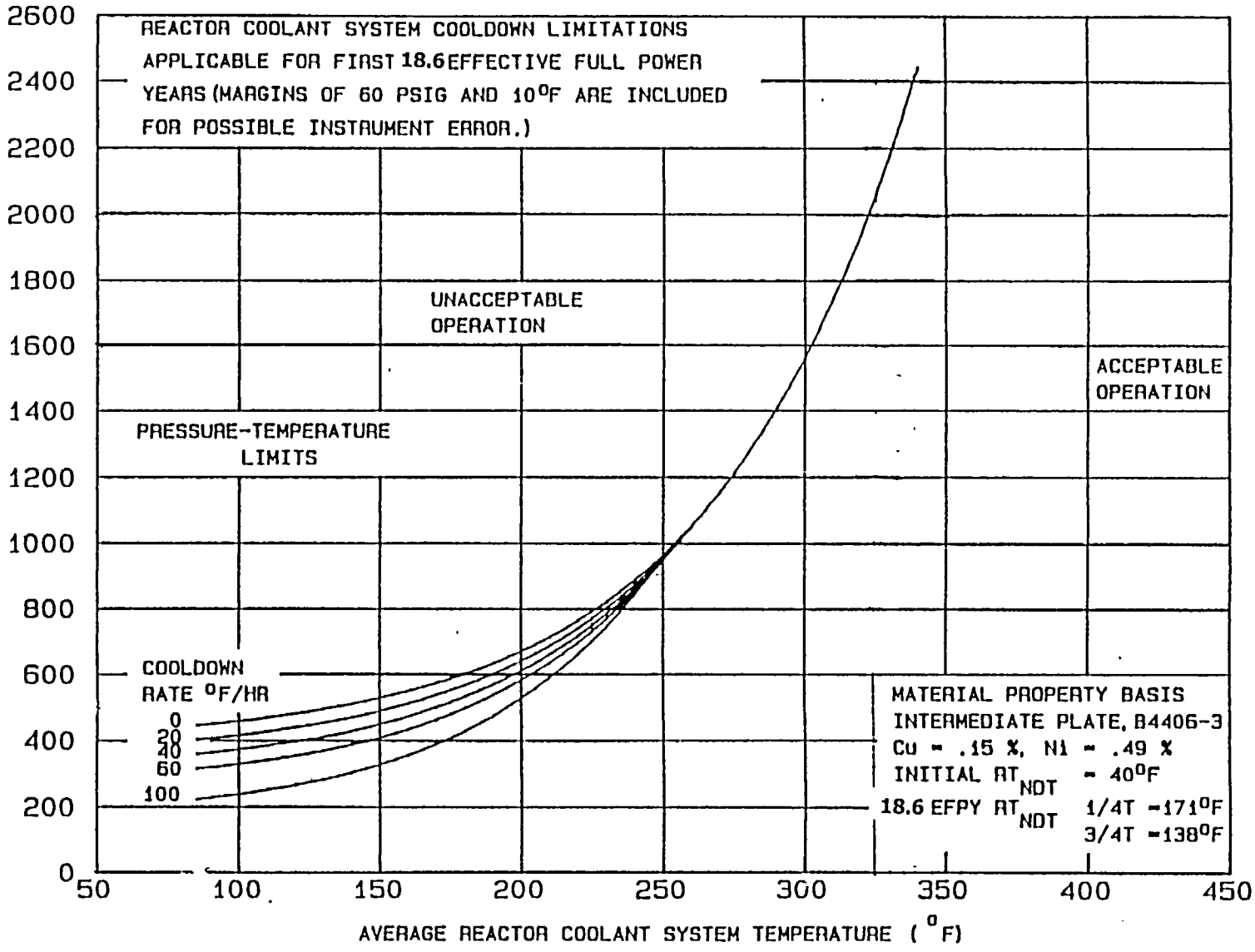

FIGURE 3.4-3

REACTOR COOLANT SYSTEM PRESSURE - TEMPERATURE LIMITS VERSUS COOLDOWN RATES

3/4.4.9 PRESSURE/TEMPERATURE LIMITS

All components in the Reactor Coolant system are designed to withstand the effects of cyclic loads due to system temperature and pressure changes. These cyclic loads are introduced by normal load transients, reactor trips, and startup and shutdown operations. The various categories of load cycles used for design purposes are provided in Section 4.1.4 of the FSAR. During startup and shutdown, the rates of temperature and pressure changes are limited so that the maximum specified heatup and cooldown rates are consistent with the design assumptions and satisfy the stress limits for cyclic operation.

An ID or OD one-quarter thickness surface flaw is postulated at the location in the vessel which is found to be the limiting case. There are several factors which influence the postulated location. The thermal induced bending stress during heatup is compressive on the inner surface while tensile on the outer surface of the vessel wall. During cooldown the bending stress profile is reversed. In addition, the material toughness is dependent upon irradiation and temperature and therefore the fluence profile through the reactor vessel wall, the rate of heatup and also the rate of cooldown influence the postulated flaw location.

The heatup limit curve, Figure 3.4-2, is a composite curve which was prepared by determining the most conservative case, with either the inside or outside wall controlling, for any heatup rate up to 60°F per hour. The cooldown limit curves of Figure 3.4-3 are composite curves which were prepared based upon the same type analysis with the exception that the controlling location is always the inside wall where the cooldown thermal gradients tend to produce tensile stresses while producing compressive stresses at the outside wall. The heatup and cooldown curves were prepared based upon the most limiting value of the predicted adjusted reference temperature at the end of 18.6 EFPY.

Reactor operation and resultant fast neutron (E > 1 Mev) irradiation will cause an increase in the RT_{NDT}. Therefore, an adjusted reference temperature, based upon the fluence, and the copper and nickel content of the material must be predicted. The heatup and cooldown limit curves of Figures 3.4-2 and 3.4-3 include the adjusted RT_{NDT} at the end of 18.6 EFPY, as well as adjustments for possible errors in the pressure and temperature sensing instruments.

The 18.6 EFPY heatup and cooldown curves were developed based on the following:

1. The intermediate shell plate, B4406-3, being the limiting material with a copper and nickel content of .15% and .49%, respectively.

2. The fluence values documented in I&M letter AEP:NRC:2900-02.

3. Figure 1, NRC Regulatory Guide 1.99, Revision 2

The shift in RT_{NDT} of the reactor vessel material has been established by removing and evaluating the material surveillance capsules installed near the inside wall of the reactor vessel in accordance with the removal schedule in Table 4.4-5. Per this schedule, Capsule U is the last capsule to be removed until Capsule S is to be removed after 32 EFPY (EOL). Capsule V, W, and Z will remain in the reactor vessel, and will be removed to address industry reactor embrittlement concerns, if required.

The pressure-temperature limit lines shown on Figure 3.4-2 for reactor criticality and for inservice leak and hydrostatic testing have been provided to assure compliance with the minimum temperature requirements of Appendix G to 10 CFR 50.

The number of reactor vessel irradiation surveillance specimens and the frequencies for removing these specimens are provided in Table 4.4-5 to assure compliance with the requirements of Appendix H to 10 CFR Part 50.

The limitations imposed on pressurizer heatup and cooldown and spray water temperature differential are provided to assure that the pressurizer is operated within the design criteria assumed for the fatigue analysis performed in accordance with the ASME Code requirements.

The OPERABILITY of two PORVs, or of one PORV and the RHR safety valve, ensures that the RCS will be protected from pressure transients which could exceed the limits of Appendix G to 10 CFR Part 50 when one or more of the RCS cold legs are less than or equal to 152°F. Either PORV or RHR safety valve has adequate relieving capability to protect the RCS from overpressurization when the transient is limited to either (1) the start of an idle RCP with the secondary water temperature of the steam generator less than or equal to 50°F above the RCS cold leg temperatures or (2) the start of a charging pump and its injection into a water solid RCS. Therefore, any one of the three blocked open PORVs constituted an acceptable RCS vent to preclude APPLICABILITY of Specification 3.4.9.3.

ATTACHMENT 3 TO AEP:NRC:2900-02

COMPUTATION OF REVISED APPLICABILITY LIMIT FOR UNIT 1 REACTOR COOLANT SYSTEM PRESSURE-TEMPERATURE CURVES

Inputs and Assumptions

- The existing curves provided as Technical Specifications (TS) Figures 3.4-2 and 3.4-3 were approved by Donald C. Cook Nuclear Plant (CNP) Unit 1 License Amendment 167 (Reference 1). Amendment 167 was based on WCAP-12483 (Reference 2), which was transmitted to the NRC by Reference 3.
- The applicability limit for the existing curves is 32 effective full-power years (EFPY).
- The peak surface fluence used in calculating adjusted reference temperature (ART) from WCAP-12483 is 1.41×10^{19} neutrons per square centimeter (n/cm^2) ($E > 1.0$ MeV).
- The Chemistry Factor (CF) of the girth weld (Heat 1P3571) is 218.6 degrees Fahrenheit (°F) [Regulatory Guide (RG) 1.99, Revision 2 (Reference 4), Position 2.1]. Indiana Michigan Power Company (I&M) has determined that the weld data is credible. The weld data was adjusted for chemistry and temperature for CNP Unit 1.
- Using surveillance capsule data CF (i.e., Reference 4, Position 2.1), 1/4 thickness ART (1/4T ART) = 171°F, 3/4 thickness ART (3/4T ART) = 138°F.
- Initial reference nil-ductility transition temperature (RT_{NDT}) of the girth weld is –56°F (Generic), thus the Margin for Credible Data is 44.0°F.
- The peak neutron fluence projections for the CNP Unit 1 Measurement Uncertainty Recapture (MUR) uprate are as indicated in the table below. These fluence projections are based on the analysis provided as Attachment 4 to this letter and assume an uprate to 3315 megawatts-thermal (MWt) at the beginning of Fuel Cycle 18.

EFPY	Peak Fluence (E >1.0 MeV)
16.68	0.8351×10^{19} n/cm^2
25	1.240×10^{19} n/cm^2
32	1.587×10^{19} n/cm^2

- The 16.68 EFPY value is the projected end-of-cycle 17 EFPY. The actual end-of-cycle 17 value was 16.64 EFPY. Therefore, this assumption is conservative.
- $ART = Margin + Initial\ RT_{NDT} + (CF \times FF)$, where FF = fluence factor (Equation. 1)

- $FF = f^{(0.28 - 0.1 \times \log(f))}$. FF is at the 1/4T or 3/4T locations, where "f" is the neutron fluence, n/cm^2 (E > 1 MeV), divided by 10^{19} (Equation 2)
- 1/4T or 3/4T Fluence @ "X" EFPY = $f_{surface}$ @ "X" EFPY × $e^{(-0.24 \times Y)}$, where "$f_{surface}$" is the clad/base metal interface surface fluence and "Y" is the depth into the vessel wall (Y = .25 or .75 times 8.5 inches). (Equation 3)

Computation

- Using Equation 1, and solving for 1/4T FF:
  1/4T ART = Initial RT_{NDT} + Margin + (CF × 1/4T FF)
  171°F = -56°F + 44°F +(218.6°F × 1/4T FF)
  Thus, 1/4T FF = 0.8371

- Using Equation 1, and solving for 3/4T FF:
  3/4T ART = Initial RT_{NDT} + Margin + (CF × 3/4T FF)
  138°F = -56°F + 44°F +(218.6°F × 3/4T FF)
  Thus, 3/4T FF = 0.6862

- Given the 1/4T FF and 3/4T FF values, and using Equation 2, neutron fluence is:
  1/4T neutron fluence = 0.5586×10^{19} n/cm^2
  3/4T neutron fluence = 0.319×10^{19} n/cm^2

- Back calculating using Equation 3, $f_{surface}$ would be either:

  $f_{surface} = 0.930 \times 10^{19}$ n/cm^2 (using the 1/4T fluence value)

  OR

  $f_{surface} = 1.473 \times 10^{19}$ n/cm^2 (using the 3/4T fluence value)

- Using the lowest $f_{surface}$ will produce the most conservative Applicability Limit (AL) when comparing to the MUR uprate fluence values. To determine the minimum AL, use the minimum fluence and interpolate the AL using the given uprated fluence projections:

AL = [16.68 + (32 - 16.68) × (Fluence @ AL - Fluence @ 16.68) / (Fluence @ 32 - Fluence @ 16.68)]

Applicability Limit = 18.62 EFPY

Conclusion

The existing reactor coolant system pressure-temperature curves in Unit 1 TS Figure 3.4-2 and TS Figure 3.4-3 are conservatively acceptable for 18.62 EFPY based on the uprated power level and considering the updated weld data adjusted for chemistry and temperature factors.

References

1. Letter from J. F. Stang, NRC, to E. E. Fitzpatrick, I&M, "Donald C. Cook Nuclear Plant, Unit 1 – Amendment No. 167 to Facility Operating License No. DPR-58 (TAC Nos. M71480 and M75260)," dated October 26, 1992

2. WCAP-12483, "Analysis of Capsule U from the American Electric Power Company D. C. Cook Unit 1 Reactor Vessel Radiation Surveillance Program," E. Terek, S. L. Anderson, L. Albertin and N. K. Ray, dated January 1990

3. Letter from M. P. Alexich, I&M, to NRC Document Control Desk, "Reactor Vessel Material Surveillance Reports," AEP:NRC:0892M, dated June 22, 1990

4. Regulatory Guide 1.99, "Radiation Embrittlement of Reactor Vessel Materials," Revision 2, dated May 1988

ATTACHMENT 4 TO AEP:NRC:2900-02

RADIATION ANALYSIS AND NEUTRON DOSIMETRY FOR THE DONALD C. COOK NUCLEAR PLANT UNIT 1 MEASUREMENT UNCERTAINTY RECAPTURE

The report provided in this Attachment 4 was generated by Westinghouse to consider the impact of data pertaining to a new limiting reactor vessel beltline material, weld heat # 1P3571, and the uprated fluence values associated with the Donald C. Cook Nuclear Power Plant (CNP) Unit 1 Measurement Uncertainty Recapture power uprate, combined, on the CNP Unit 1 pressure-temperature curves. This report was reviewed and owner-accepted by Indiana Michigan Power Company and is unchanged in style and substance from the original Westinghouse report.

RADIATION ANALYSIS AND NEUTRON DOSIMETRY
FOR THE D. C. COOK UNIT 1 MUR

1. Introduction

This report describes a discrete ordinates S_n transport analysis performed for the D. C. Cook Unit 1 reactor to determine the neutron radiation environment within the reactor pressure vessel and surveillance capsules. In this evaluation, fast neutron exposure parameters in terms of fast neutron fluence (E > 1.0 MeV) and iron atom displacements (dpa) were established on a plant and fuel cycle specific basis for the first seventeen reactor operating cycles. In addition, neutron dosimetry sensor sets from Surveillance Capsules T, X, Y, and U withdrawn from the D. C. Cook Unit 1 reactor at the conclusion of fuel cycles 1, 4, 6, and 10 were analyzed using current dosimetry evaluation methodology. Comparisons of the results of these dosimetry evaluations with the analytical predictions provided a validation of the plant specific neutron transport calculations. These validated calculations were then used to provide projections of the neutron exposure of the reactor pressure vessel for operating periods extending to 54 Effective Full Power Years (EFPY). These projections were based on the assumption that the spatial power distribution for cycle seventeen is representative of future plant operation. The future projections also account for a power uprate from 3250 MWt to 3315 MWt at the onset of cycle eighteen. All of the neutron transport calculations and dosimetry evaluations described in this section meet the requirements of Regulatory Guide 1.190, "Calculational and Dosimetry Methods for Determining Pressure Vessel Neutron Fluence."[1]

The use of fast neutron fluence (E > 1.0 MeV) to correlate measured material property changes to the neutron exposure of the material has traditionally been accepted for the development of damage trend curves as well as for the implementation of trend curve data to assess the condition of the vessel. In recent years; however, as discussed in Regulatory Guides 1.190 and 1.99, Revision 2, an exposure model that accounts for differences in neutron energy spectra between surveillance capsule locations and positions within the vessel wall could lead to an improvement in the uncertainties associated with damage trend curves and improved accuracy in the evaluation of damage gradients through the reactor vessel wall.

Because of this potential shift away from a threshold fluence toward an energy dependent damage function for data correlation, ASTM Standard Practice E853, "Analysis and Interpretation of Light-Water Reactor Surveillance Results," recommends reporting displacements per iron atom (dpa) along with fluence (E > 1.0 MeV) to provide a database for future reference. The energy dependent dpa function to be used for this evaluation is specified in ASTM Standard Practice E693, "Characterizing Neutron Exposures in Iron and Low Alloy Steels in Terms of Displacements per Atom." The application of the dpa parameter to the assessment of embrittlement gradients through the thickness of the reactor vessel wall has already been promulgated in Revision 2 to Regulatory Guide 1.99, "Radiation Embrittlement of Reactor Vessel Materials."

All of the calculations and dosimetry evaluations described in this section were based on the latest available nuclear cross-section data derived from ENDF/B-VI and made use of the latest available calculational tools. Additionally, the methods used to develop the calculated pressure vessel fluence are consistent with the NRC approved methodology described in WCAP-14040-NP-A, "Methodology Used to Develop Cold Overpressure Mitigating System Setpoints and RCS Heatup and Cooldown Limit Curves," January 1996.[2] The specific calculational methods applied are also consistent with those

described in WCAP-15557, "Qualification of the Westinghouse Pressure Vessel Neutron Fluence Evaluation Methodology."[3]

It should be noted that because the neutron dosimetry sets from the first four surveillance capsules were re-analyzed herein using current dosimetry evaluation methodology, the results do not exactly match those reported in Reference 6.

2. Discrete Ordinates Analysis

Eight irradiation capsules attached to the thermal shield are included in the D. C. Cook Unit 1 reactor design that constitutes the reactor vessel surveillance program. The capsules are located at azimuthal angles of 4°, 176°, 184°, 356° (4° from the core cardinal axes) and 40°, 140°, 220°, 320° (40° from the core cardinal axes). The stainless steel specimen containers are 1-inch square and approximately 38 inches in height. The containers are positioned axially such that the test specimens are centered on the core midplane, thus spanning the central 3 feet of the 12-foot high reactor core. Capsules T, X, Y, and U were originally loaded into the 40° azimuthal location, while Capsules S, V, W, and Z were positioned at 4°. Capsules T, X, Y and U were withdrawn for analysis at the conclusion of the first, fourth, sixth, and tenth fuel cycles, respectively. After fuel cycle fourteen, Capsule S was re-positioned from the 4° to the 40° location. At this time, the capsule was re-designated as Capsule W, while the original Capsule W was re-designated Capsule S (Reference 4). The irradiation history of each of these eight surveillance capsules is summarized as follows:

Capsule	Location	Irradiation History
T	40°	Cycle 1 (withdrawn for analysis)
X	40°	Cycles 1-4 (withdrawn for analysis)
Y	40°	Cycles 1-6 (withdrawn for analysis)
U	40°	Cycles 1-10 (withdrawn for analysis)
S(1)	4°	Cycles 1-17 (in reactor)
V	4°	Cycles 1-17 (in reactor)
W(1)	4°/40°	Cycles 1-17 (in reactor)
Z	4°	Cycles 1-17 (in reactor)

Note:

1. Capsule W was formally located at the 4° position and known as Capsule S. Capsule S was formally known as Capsule W. These changes are documented in Reference 4.

From a neutronic standpoint, the surveillance capsules and associated support structures are significant. The presence of these materials has a marked effect on both the spatial distribution of neutron flux and the neutron energy spectrum in the water annulus between the thermal shield and the reactor vessel. In order to determine the neutron environment at the test specimen location, the capsules themselves must be included in the analytical model.

The fast neutron exposure evaluations for the D. C. Cook Unit 1 surveillance capsules and reactor vessel were based on a series of duel cycle specific forward transport calculations that were combined using the following three-dimensional flux synthesis technique:

$$\phi(r,\theta,z) = [\phi(r,\theta)] * [\phi(r,z)]/[\phi(r)]$$

where $\phi(r,\theta,z)$ is the synthesized three-dimensional neutron flux distribution, $\phi(r,\theta)$ is the transport solution in r,θ geometry, $\phi(r,z)$ is the two-dimensional solution for a cylindrical reactor model using the actual axial core power distribution, and $\phi(r)$ is the one-dimensional solution for a cylindrical reactor model using the same source per unit height as that used in the r,θ two-dimensional calculation. This synthesis procedure was carried out for each operating cycle at D. C. Cook Unit 1.

For the D. C. Cook Unit 1 calculations, one r,θ model was developed since the reactor is octant symmetric. This r,θ model includes the core, the reactor internals, the thermal shield - including explicit representations of the surveillance capsules at 4° and 40°, the pressure vessel cladding and vessel wall, the insulation external to the pressure vessel, and the primary biological shield wall. The symmetric r,θ model was utilized to perform both the surveillance capsule dosimetry evaluations, and subsequent comparisons with calculated results, and to generate the maximum fluence levels at the pressure vessel wall. In developing this analytical model, nominal design dimensions were employed for the various structural components. Likewise, water temperatures, and hence, coolant densities in the reactor core and downcomer regions of the reactor were taken to be representative of full power operating conditions. The coolant densities were treated on a fuel cycle specific basis. The reactor core itself was treated as a homogeneous mixture of fuel, cladding, water, and miscellaneous core structures such as fuel assembly grids, guide tubes, et cetera. The r,θ geometric mesh description of the reactor model consisted of 170 radial by 67 azimuthal intervals. Mesh sizes were chosen to assure that proper convergence of the inner iterations was achieved on a pointwise basis. The pointwise inner iteration flux convergence criterion utilized in the r,θ calculations was set at a value of 0.001.

The r,z model used for the D. C. Cook Unit 1 calculations extended radially from the centerline of the reactor core out to a location interior to the primary biological shield and over an axial span from an elevation 1-foot below the active fuel to 1-foot above the active fuel. As in the case of the r,θ model, nominal design dimensions and full power coolant densities were employed in the calculations. In this case, the homogenous core region was treated as an equivalent cylinder with a volume equal to that of the active core zone. The stainless steel former plates located between the core baffle and core barrel regions were also explicitly included in the model. The r,z geometric mesh description of the reactor model consisted of 153 radial by 90 axial intervals. As in the case of the r,θ calculations, mesh sizes were chosen to assure that proper convergence of the inner iterations was achieved on a pointwise basis. The pointwise inner iteration flux convergence criterion utilized in the r,z calculations was also set at a value of 0.001.

The one-dimensional radial model used in the synthesis procedure consisted of the same 153 radial mesh intervals included in the r,z model. Thus, radial synthesis factors could be determined on a meshwise basis throughout the entire geometry.

The core power distributions for the first seven fuel cycles used in the plant specific transport analysis were obtained from Reference 5 (which was the input used in the previous surveillance capsule analysis, documented in Reference 6). The core power distributions for cycles eight through seventeen were taken from the appropriate D. C. Cook Unit 1 fuel cycle design reports (References 7 through 16). The data extracted from the references represented cycle dependent fuel assembly enrichments, burnups, and axial power distributions. This information was used to develop spatial and energy dependent core source distributions averaged over each individual fuel cycle. Therefore, the results from the neutron transport calculations provided data in terms of fuel cycle averaged neutron flux, which when multiplied by the appropriate fuel cycle length, generated the incremental fast neutron exposure for each fuel cycle. The

individual cycle lengths used in these calculations differ slightly from the AEP provided design input. These differences were evaluated and found to be insignificant.

In constructing these core source distributions, the energy distribution of the source was based on an appropriate fission split for uranium and plutonium isotopes based on the initial enrichment and burnup history of individual fuel assemblies. From these assembly dependent fission splits, composite values of energy release per fission, neutron yield per fission, and fission spectrum were determined. The spatial power distributions used in the transport analyses are provided in Appendix A to this report.

All of the transport calculations supporting this analysis were carried out using the DORT discrete ordinates code Version 3.1[17] and the BUGLE-96 cross-section library.[18] The BUGLE-96 library provides a 67 group coupled neutron-gamma ray cross-section data set produced specifically for light water reactor (LWR) applications. In these analyses, anisotropic scattering was treated with a P_5 legendre expansion and angular discretization was modeled with an S_{16} order of angular quadrature. Energy and space dependent core power distributions, as well as system operating temperatures, were treated on a fuel cycle specific basis.

Selected results from the neutron transport analyses are provided in Tables 1 through 4. The data listed in these tables establish the means for absolute comparisons of analysis and measurement for the Capsules T, X, Y, and U irradiation and provide the calculated neutron exposure of the pressure vessel wall for the first seventeen fuel cycles. In Table 1, the calculated exposure rates and integrated exposures, expressed in terms of both neutron fluence (E > 1.0 MeV) and dpa, are given at the radial and azimuthal center of the two azimuthally symmetric surveillance capsule positions (4° and 40°). These data, representative of the axial midplane of the active core, are meant to establish the exposure of the surveillance capsules withdrawn to date and to provide an absolute comparison of measurement with calculation. Similar information is provided in Table 2 for the reactor vessel inner radius. The vessel data given in Table 2 are representative of the axial location of the maximum neutron exposure at each of the four azimuthal locations. Again, both fluence (E > 1.0 MeV) and dpa data are provided. It is important to note that the data for the vessel inner radius were taken at the clad/base metal interface, and thus, represent the maximum calculated exposure levels of the vessel plates and welds.

Radial gradient information applicable to ϕ(E > 1.0 MeV) and dpa/sec are given in Tables 3 and 4, respectively. The data, based on the Cycles 1 through 17 cumulative fluence, are presented on a relative basis for each exposure parameter at several azimuthal locations. Exposure distributions through the vessel wall may be obtained by multiplying the calculated exposure at the vessel inner radius by the gradient data listed in Tables 3 and 4.

3. Neutron Dosimetry

3.1 Sensor Reaction Rate Determinations

In this section, the results of the evaluations of the four neutron sensor sets withdrawn to date as a part of the D. C. Cook Unit 1 Reactor Vessel Materials Surveillance Program are presented. The capsule designation, location within the reactor, and time of withdrawal of each of these dosimetry sets were as follows:

Capsule ID	Azimuthal Location	Withdrawal Time	Irradiation Time [EFPY]
T	40°	End of Cycle 1	1.27
X	40°	End of Cycle 4	3.48
Y	40°	End of Cycle 6	4.95
U	40°	End of Cycle 10	9.17

The azimuthal locations included in the above tabulation represent the first octant equivalent azimuthal angle of the geometric center of the respective surveillance capsules.

The passive neutron sensors included in the evaluations of Surveillance Capsules T, X, Y, and U are summarized as follows:

Sensor Material	Reaction of Interest	Capsule T	Capsule X	Capsule Y	Capsule U
Copper	$^{63}Cu(n,\alpha)^{60}Co$	X	X	X	X
Iron	$^{54}Fe(n,p)^{54}Mn$	X	X	X	X**
Nickel	$^{58}Ni(n,p)^{58}Co$	X	X	X	X
Uranium-238	$^{238}U(n,f)^{137}Cs$	X	X	X	X
Neptunium-237	$^{237}Np(n,f)^{137}Cs$	X	X	X	X
Cobalt-Aluminum*	$^{59}Co(n,\gamma)^{60}Co$	X	X	X	X

* The cobalt-aluminum measurements for this plant include both bare wire and cadmium-covered sensors

** One of the five iron sensors in Capsule U was not recovered.

The copper, iron, nickel, and cobalt-aluminum monitors, in wire form, were placed in holes drilled in spacers at several radial locations within the test specimen array. As a result, gradient corrections were applied to these measured reaction rates in order to index all of the sensor measurements to the radial center of the respective surveillance capsules. Since the cadmium-shielded uranium and neptunium fission monitors were accommodated within the dosimeter block centered at the radial, azimuthal, and axial center of the material test specimen array, gradient corrections were not required for the fission monitor reaction rates. Pertinent physical and nuclear characteristics of the passive neutron sensors are listed in Table 5.

The use of passive monitors such as those listed above does not yield a direct measure of the energy dependent neutron flux at the point of interest. Rather, the activation or fission process is a measure of the integrated effect that the time and energy dependent neutron flux has on the target material over the course of the irradiation period. An accurate assessment of the average neutron flux level incident on the various monitors may be derived from the activation measurements only if the irradiation parameters are well known. In particular, the following variables are of interest:

- the measured specific activity of each monitor,
- the physical characteristics of each monitor,
- the operating history of the reactor,
- the energy response of each monitor, and
- the neutron energy spectrum at the monitor location.

The radiometric counting of the neutron sensors from Capsules T, X, and Y was carried out at the Southwest Research Institute (SwRI). The radiometric counting of the sensors from Capsule U was completed at the Westinghouse Analytical Laboratory, located at the Waltz Mill Site. In all cases, the radiometric counting followed established ASTM procedures. Following sample preparation and weighing, the specific activity of each sensor was determined by means of a high-resolution gamma spectrometer. For the copper, iron, nickel, and cobalt-aluminum sensors, these analyses were performed by direct counting of each of the individual samples. In the case of the uranium and neptunium fission sensors, the analyses were carried out by direct counting preceded by dissolution and chemical separation of cesium from the sensor material.

The irradiation history of the reactor over the irradiation periods experienced by Capsules T, X, Y, and U was based on the reported monthly power generation of D. C. Cook Unit 1 from initial reactor startup through the end of the dosimetry evaluation period. For the sensor sets utilized in the surveillance capsules, the half-lives of the product isotopes are long enough that a monthly histogram describing reactor operation has proven to be an adequate representation for use in radioactive decay corrections for the reactions of interest in the exposure evaluations. The irradiation history applicable to Capsules T, X, Y, and U is given in Table 6.

Having the measured specific activities, the physical characteristics of the sensors, and the operating history of the reactor, reaction rates referenced to full-power operation were determined from the following equation:

$$R = \frac{A}{N_0 \, F \, Y \, \Sigma \, \frac{P_j}{P_{ref}} \, C_j \, [1 - e^{-\lambda t_j}] \, [e^{-\lambda t_d}]}$$

where:

R	=	Reaction rate averaged over the irradiation period and referenced to operation at a core power level of P_{ref} (rps/nucleus).
A	=	Measured specific activity (dps/gm).
N_0	=	Number of target element atoms per gram of sensor.
F	=	Weight fraction of the target isotope in the sensor material.
Y	=	Number of product atoms produced per reaction.
P_j	=	Average core power level during irradiation period j (MW).
P_{ref}	=	Maximum or reference power level of the reactor (MW).
C_j	=	Calculated ratio of $\phi(E > 1.0 \text{ MeV})$ during irradiation period j to the time weighted average $\phi(E > 1.0 \text{ MeV})$ over the entire irradiation period.
λ	=	Decay constant of the product isotope (1/sec).
t_j	=	Length of irradiation period j (sec).
t_d	=	Decay time following irradiation period j (sec).

and the summation is carried out over the total number of monthly intervals comprising the irradiation period.

In the equation describing the reaction rate calculation, the ratio $[P_j]/[P_{ref}]$ accounts for month-by-month variation of reactor core power level within any given fuel cycle as well as over multiple fuel cycles. The ratio C_j, which was calculated for each fuel cycle using the transport methodology discussed in Section 2, accounts for the change in sensor reaction rates caused by variations in flux level induced by changes in core spatial power distributions from fuel cycle to fuel cycle. For a single-cycle irradiation, C_j is normally taken to be 1.0. However, for multiple-cycle irradiations, particularly those employing low leakage fuel management, the additional C_j term should be employed. The impact of changing flux levels for constant power operation can be quite significant for sensor sets that have been irradiated for many cycles in a reactor that has transitioned from non-low leakage to low leakage fuel management or for sensor sets contained in surveillance capsules that have been moved from one capsule location to another. The fuel cycle specific neutron flux values along with the computed values for C_j are listed in Table 7. These flux values represent the cycle dependent results at the radial and azimuthal center of the respective capsules at the axial elevation of the active fuel midplane.

Prior to using the measured reaction rates in the least-squares evaluations of the dosimetry sensor sets, additional corrections were made to the ^{238}U measurements to account for the presence of ^{235}U impurities in the sensors as well as to adjust for the build-in of plutonium isotopes over the course of the irradiation. Corrections were also made to the ^{238}U and ^{237}Np sensor reaction rates to account for gamma ray induced fission reactions that occurred over the course of the capsule irradiations. The correction factors applied to the D. C. Cook Unit 1 fission sensor reaction rates are summarized as follows:

Correction	Capsule T	Capsule X	Capsule Y	Capsule U
^{235}U Impurity/Pu Build-in	0.874	0.853	0.838	0.815
$^{238}U(\gamma,f)$	0.958	0.958	0.958	0.958
Net ^{238}U Correction	0.837	0.817	0.803	0.780
$^{237}Np(\gamma,f)$	0.985	0.985	0.985	0.985

These factors were applied in a multiplicative fashion to the decay corrected uranium and neptunium fission sensor reaction rates.

Results of the sensor reaction rate determinations for Capsules T, X, Y, and U are given in Table 8. In Table 8, the measured specific activities, decay corrected saturated specific activities, and computed reaction rates for each sensor indexed to the radial center of the capsule are listed. The fission sensor reaction rates are listed both with and without the applied corrections for ^{238}U impurities, plutonium build-in, and gamma ray induced fission effects.

In regard to the data listed in Table 8, it should be noted that the reaction rates obtained for the fission monitors from Capsule T were significantly higher than would be expected for this capsule configuration and irradiation history. Similarly, the reaction rates for obtained for the fission monitors from Capsule U were significantly lower than would be expected for this capsule configuration and irradiation history. These observations are based on comparison of the reaction rates for these fission monitors with data obtained from other 40° surveillance capsule irradiations at 4-loop plants. Because of this, the data for these fission monitors was not used in the least squares analyses of Capsules T and U.

3.2 Least Squares Evaluation of Sensor Sets

Least squares adjustment methods provide the capability of combining the measurement data with the corresponding neutron transport calculations resulting in a Best Estimate neutron energy spectrum with associated uncertainties Best Estimates for key exposure parameters such as $\phi(E > 1.0\ MeV)$ or dpa/s

along with their uncertainties are then easily obtained from the adjusted spectrum. In general, the least squares methods, as applied to surveillance capsule dosimetry evaluations, act to reconcile the measured sensor reaction rate data, dosimetry reaction cross-sections, and the calculated neutron energy spectrum within their respective uncertainties. For example,

$$R_i \pm \delta_{R_i} = \sum_g (\sigma_{ig} \pm \delta_{\sigma_{ig}})(\phi_g \pm \delta_{\phi_g})$$

relates a set of measured reaction rates, R_i, to a single neutron spectrum, ϕ_g, through the multigroup dosimeter reaction cross-section, σ_{ig}, each with an uncertainty δ. The primary objective of the least squares evaluation is to produce unbiased estimates of the neutron exposure parameters at the location of the measurement.

For the least squares evaluation of the D. C. Cook Unit 1 surveillance capsule dosimetry, the FERRET code[19] was employed to combine the results of the plant specific neutron transport calculations and sensor set reaction rate measurements to determine best-estimate values of exposure parameters ($\phi(E > 1.0$ MeV) and dpa) along with associated uncertainties for the four in-vessel capsules withdrawn to date.

The application of the least squares methodology requires the following input:

1 - The calculated neutron energy spectrum and associated uncertainties at the measurement location.

2 - The measured reaction rates and associated uncertainty for each sensor contained in the multiple foil set.

3 - The energy dependent dosimetry reaction cross-sections and associated uncertainties for each sensor contained in the multiple foil sensor set.

For the D. C. Cook Unit 1 application, the calculated neutron spectrum was obtained from the results of plant specific neutron transport calculations described in Section 2 of this report. The sensor reaction rates were derived from the measured specific activities using the procedures described in Section 3.1. The dosimetry reaction cross-sections and uncertainties were obtained from the Sandia National Laboratory Radiation Metrology Laboratory (SNLRML) dosimetry cross-section library[20]. The SNLRML library is an evaluated dosimetry reaction cross-section compilation recommended for use in LWR evaluations by ASTM Standard E1018, "Application of ASTM Evaluated Cross-Section Data File, Matrix E 706 (IIB)."

The uncertainties associated with the measured reaction rates, dosimetry cross-sections, and calculated neutron spectrum were input to the least squares procedure in the form of variances and covariances. The assignment of the input uncertainties followed the guidance provided in ASTM Standard E 944, "Application of Neutron Spectrum Adjustment Methods in Reactor Surveillance."

The following provides a summary of the uncertainties associated with the least squares evaluation of the D. C. Cook Unit 1 surveillance capsule sensor sets.

Reaction Rate Uncertainties

The overall uncertainty associated with the measured reaction rates includes components due to the basic measurement process, irradiation history corrections, and corrections for competing reactions. A high level of accuracy in the reaction rate determinations is assured by utilizing laboratory procedures that conform to the ASTM National Consensus Standards for reaction rate determinations for each sensor type.

After combining all of these uncertainty components, the sensor reaction rates derived from the counting and data evaluation procedures were assigned the following net uncertainties for input to the least squares evaluation:

Reaction	Uncertainty
$^{63}Cu(n,\alpha)^{60}Co$	5%
$^{54}Fe(n,p)^{54}Mn$	5%
$^{58}Ni(n,p)^{58}Co$	5%
$^{238}U(n,f)^{137}Cs$	10%
$^{237}Np(n,f)^{137}Cs$	10%
$^{59}Co(n,\gamma)^{60}Co$	5%

These uncertainties are given at the 1σ level.

Dosimetry Cross-Section Uncertainties

The reaction rate cross-sections used in the least squares evaluations were taken from the SNLRML library. This data library provides reaction cross-sections and associated uncertainties, including covariances, for 66 dosimetry sensors in common use. Both cross-sections and uncertainties are provided in a fine multigroup structure for use in least squares adjustment applications. These cross-sections were compiled from the most recent cross-section evaluations and they have been tested with respect to their accuracy and consistency for least squares evaluations. Further, the library has been empirically tested for use in fission spectra determination as well as in the fluence and energy characterization of 14 MeV neutron sources.

For sensors included in the D. C. Cook Unit 1 surveillance program, the following uncertainties in the fission spectrum averaged cross-sections are provided in the SNLRML documentation package.

Reaction	Uncertainty
$^{63}Cu(n,\alpha)^{60}Co$	4.08-4.16%
$^{54}Fe(n,p)^{54}Mn$	3.05-3.11%
$^{58}Ni(n,p)^{58}Co$	4.49-4.56%
$^{238}U(n,f)^{137}Cs$	0.54-0.64%
$^{237}Np(n,f)^{137}Cs$	10.32-10.97%
$^{59}Co(n,\gamma)^{60}Co$	0.79-3.59%

These tabulated ranges provide an indication of the dosimetry cross-section uncertainties associated with the sensor sets used in LWR irradiations.

Calculated Neutron Spectrum

The neutron spectra input to the least squares adjustment procedure were obtained directly from the results of plant specific transport calculations for each surveillance capsule irradiation period and location. The spectrum for each capsule was input in an absolute sense (rather than as simply a relative spectral shape). Therefore, within the constraints of the assigned uncertainties, the calculated data were treated equally with the measurements.

While the uncertainties associated with the reaction rates were obtained from the measurement procedures and counting benchmarks and the dosimetry cross-section uncertainties were supplied directly with the SNLRML library, the uncertainty matrix for the calculated spectrum was constructed from the following relationship:

$$M_{gg'} = R_n^2 + R_g * R_{g'} * P_{gg'}$$

where R_n specifies an overall fractional normalization uncertainty and the fractional uncertainties R_g and $R_{g'}$ specify additional random groupwise uncertainties that are correlated with a correlation matrix given by:

$$P_{gg'} = [1-\theta]\delta_{gg'} + \theta e^{-H}$$

where

$$H = \frac{(g-g')^2}{2\gamma^2}$$

The first term in the correlation matrix equation specifies purely random uncertainties, while the second term describes the short-range correlations over a group range γ (θ specifies the strength of the latter term). The value of δ is 1.0 when g = g', and is 0.0 otherwise.

The set of parameters defining the input covariance matrix for the D. C. Cook Unit 1 calculated spectra was as follows:

Flux Normalization Uncertainty (R_n)	15%
Flux Group Uncertainties (R_g, $R_{g'}$)	
(E > 0.0055 MeV)	15%
(0.68 eV < E < 0.0055 MeV)	29%
(E < 0.68 eV)	52%
Short Range Correlation (θ)	
(E > 0.0055 MeV)	0.9
(0.68 eV < E < 0.0055 MeV)	0.5
(E < 0.68 eV)	0.5
Flux Group Correlation Range (γ)	
(E > 0.0055 MeV)	6
(0.68 eV < E < 0.0055 MeV)	3
(E < 0.68 eV)	2

3.3 Comparisons of Measurements and Calculations

Results of the least squares evaluations of the dosimetry from the four D. C. Cook Unit 1 surveillance capsules withdrawn to date are provided in Tables 9 and 10. In Table 9, measured, calculated, and best-estimate values for sensor reaction rates are given for each capsule. The best estimate values represent the adjusted values resulting from the least squares evaluation of the calculations and measurements. Also provided in this tabulation are ratios of the measured reaction rates to both the calculated and least squares adjusted reaction rates (best estimate). These ratios of M/C and M/BE illustrate the consistency of the fit of the calculated neutron energy spectra to the measured reaction rates both before and after adjustment. In Table 10, comparison of the calculated and best estimate values of neutron flux (E > 1.0 MeV) and iron atom displacement rate are tabulated along with the BE/C ratios observed for each of the capsules.

The data comparisons provided in Tables 9 and 10 show that the adjustments to the calculated spectra are relatively small and well within the assigned uncertainties for the calculated spectra, measured sensor reaction rates, and dosimetry reaction cross-sections. Further, these results indicate that the use of the least squares evaluation results in a reduction in the uncertainties associated with the exposure of the surveillance capsules. It may be noted that the uncertainty associated with the unadjusted calculation of neutron fluence (E > 1.0 MeV) and iron atom displacements at the surveillance capsule locations is specified as 12% at the 1σ level. From Table 10, it is noted that the corresponding uncertainties associated with the least squares adjusted exposure parameters have been reduced to 6-7% for neutron flux (E > 1.0 MeV) and 7-9% for iron atom displacement rate. Again, the uncertainties from the least squares evaluation are at the 1σ level.

Further comparisons of the measurement results with calculations are given in Tables 11 and 12. These comparisons are given on two levels. In Table 11, calculations of individual threshold sensor reaction rates are compared directly with the corresponding measurements. These threshold reaction rate comparisons provide a good evaluation of the accuracy of the fast neutron portion of the calculated energy spectra. In Table 12, calculations of fast neutron exposure rates in terms of ϕ(E > 1.0 MeV) and dpa/s are compared with the best estimate results obtained from the least squares evaluation of the four capsule dosimetry results. These two levels of comparison yield consistent and similar results with all measurement-to-unadjusted calculation comparisons falling well within the 20% limits specified as the acceptance criteria in Regulatory Guide 1.190.

In the case of the direct comparison of measured and calculated sensor reaction rates, only one of the measurement foil reaction rates differs from the corresponding calculated value by more than 20% (Cu-63 from Capsule T). The M/C comparisons for the other fifteen fast neutron reactions range from 0 89–1.17. The overall average M/C ratio for the entire set of D. C. Cook Unit 1 data is 1.06 with an associated standard deviation of 8.7%.

In the comparisons of best estimate and calculated fast neutron exposure parameters, the corresponding BE/C comparisons for the four capsule data set range from 0.93–1.11 for neutron flux (E > 1.0 MeV) and from 0.93 to 1.08 for iron atom displacement rate. The overall average BE/C ratios for neutron flux (E > 1.0 MeV) and iron atom displacement rate are 1.03 with a standard deviation of 7.2% and 1.02 with a standard deviation of 6.5%, respectively.

Based on these comparisons, it is concluded that the calculated fast neutron exposures provided in Section 4 of this report are validated for use in the assessment of the condition of the materials comprising the beltline region of the D. C. Cook Unit 1 reactor pressure vessel.

The uncertainty associated with the calculated neutron exposure of the D. C. Cook Unit 1 surveillance capsule and reactor pressure vessel is based on the recommended approach provided in Regulatory Guide 1.190. In particular, the qualification of the methodology was carried out in the following four stages:

1 - Comparison of calculations with benchmark measurements from the Pool Critical Assembly (PCA) simulator at the Oak Ridge National Laboratory (ORNL).

2 - Comparisons of calculations with surveillance capsule and reactor cavity measurements from the H. B. Robinson power reactor benchmark experiment.

3 - An analytical sensitivity study addressing the uncertainty components resulting important input parameters applicable to the plant specific transport calculations used in the neutron exposure assessments.

4 - Comparisons of the plant specific calculations with all available dosimetry results from the D. C. Cook Unit 1 surveillance program.

The first phase of the methods qualification (PCA comparisons) addressed the adequacy of basic transport calculation and dosimetry evaluation techniques and associated cross-sections. This phase, however, did not test the accuracy of commercial core neutron source calculations nor did it address uncertainties in operational or geometric variables that impact power reactor calculations. The second phase of the qualification (H. B. Robinson comparisons) addressed uncertainties in these additional areas that are primarily methods related and would tend to apply generically to all fast neutron exposure evaluations. The third phase of the qualification (analytical sensitivity study) identified the potential uncertainties introduced into the overall evaluation due to calculational methods approximations as well as to a lack of knowledge relative to various plant specific input parameters. The overall calculational uncertainty applicable to the D. C. Cook Unit 1 analysis was established from results of these three phases of the methods qualification.

The fourth phase of the uncertainty assessment (comparisons with D. C. Cook Unit 1 measurements) was used solely to demonstrate the validity of the transport calculations and to confirm the uncertainty estimates associated with the analytical results. It should be noted that the measured reaction rates and adjusted values of neutron flux ($E > 1.0$ MeV) and iron atom displacement rate have been used only to validate the calculated results and associated calculational uncertainty. They have not been used to modify the calculated results in any way.

The following summarizes the uncertainties developed from the first three phases of the methodology qualification. Additional information pertinent to these evaluations is provided in Reference 3.

	Capsule	Vessel IR
PCA Comparisons	3%	3%
H. B. Robinson Comparisons	3%	3%
Analytical Sensitivity Studies	10%	11%
Additional Uncertainty for Factors not Explicitly Evaluated	5%	5%
Net Calculational Uncertainty	12%	13%

The net calculational uncertainty was determined by combining the individual components in quadrature. Therefore, the resultant uncertainty was random and no systematic bias was applied to the analytical results.

The plant specific measurement comparisons provided in Tables 11 and 12 support these uncertainty assessments for D. C. Cook Unit 1.

4. Projections of Reactor Vessel Exposure

The final results of the fluence evaluations performed for the four surveillance capsules withdrawn from the D. C. Cook Unit 1 reactor are provided in Table 13. These assigned neutron exposure levels are based on the plant and fuel cycle specific neutron transport calculations performed for the D. C. Cook Unit 1 reactor. As shown by the comparisons provided in Tables 11 and 12, the validity of these calculated fluence levels is demonstrated both by a direct comparison with measured sensor reaction rates as well by comparison with the least squares evaluation performed for each of the capsule dosimetry sets.

The corresponding calculated fast neutron fluence (E > 1.0 MeV) and dpa exposure values for the D. C. Cook Unit 1 pressure vessel are provided in Table 14. As presented, these data represent the maximum exposure of the clad/base metal interface at azimuthal angles of 0, 15, 30, and 45 degrees relative to the core cardinal axes. The data tabulation includes the plant and fuel cycle specific calculated fluence at the end of cycle sixteen (the last cycle completed at the D. C. Cook Unit 1 plant), a projection to the end of cycle seventeen (the current operating cycle) and further projections for future operation to 25, 32, 36, 48, and 54 effective full power years.

The projection to the completion of cycle seventeen was based on the cycle seventeen design power distribution provided in Appendix C, continued operation at a core power level of 3250 MWt, and a design cycle length of 1.45 effective full power years. Projections beyond the end of cycle seventeen were based on the assumption that the spatial core power distribution from the cycle seventeen design is representative of future fuel cycles. It was further assumed that, for cycles eighteen and beyond, the core power level would be uprated to 3315 MWt. Therefore, the fluence projections for future operation at D. C. Cook Unit 1 are based on the assumption of a constant neutron flux at the surveillance capsule and pressure vessel locations for the operating period between 16.68 and 54 effective full power years. As required by Regulatory Guide 1.190 and as mentioned in the previous section, no bias or uncertainty is applied to the calculated results.

Updated lead factors for the D. C. Cook Unit 1 surveillance capsules are provided in Table 15. The capsule lead factor is defined as the ratio of the calculated fluence (E > 1.0 MeV) at the geometric center of the surveillance capsule to the corresponding maximum calculated fluence at the pressure vessel clad/base metal interface. In Table 15, the lead factors for capsules that have been withdrawn from the

reactor (T, X, Y, and U) were based on the calculated fluence values for the irradiation period corresponding to the time of withdrawal for the individual capsules.

Table 1

Calculated Neutron Exposure Rates and Integrated Exposures
at the Surveillance Capsule Center

Neutrons (E > 1.0 MeV)

Cycle	Cycle Length [EFPY]	Total Irradiation Time [EFPY]	Neutron Flux (E > 1.0 MeV) [n/cm^2-s]		Neutron Fluence (E > 1.0 MeV) [n/cm^2]	
			4 Degrees	40 Degrees	4 Degrees	40 Degrees
1	1.27	1.27	2.099E+10	6.674E+10	8.386E+17	2.667E+18
2	0.78	2.04	2.453E+10	8.360E+10	1.440E+18	4.718E+18
3	0.70	2.75	2.349E+10	8.069E+10	1.963E+18	6.512E+18
4	0.73	3.48	2.270E+10	7.776E+10	2.488E+18	8.313E+18
5	0.74	4.22	2.287E+10	8.106E+10	3.023E+18	1.021E+19
6	0.72	4.95	2.290E+10	7.634E+10	3.545E+18	1.195E+19
7	0.73	5.67	2.301E+10	7.689E+10	4.072E+18	1.371E+19
8	1.12	6.80	2.266E+10	4.301E+10	4.876E+18	1.524E+19
9	1.19	7.98	2.183E+10	4.214E+10	5.696E+18	1.682E+19
10	1.19	9.17	1.936E+10	4.151E+10	6.422E+18	1.837E+19
11	1.14	10.32	1.934E+10	4.215E+10	7.119E+18	1.989E+19
12	1.19	11.51	1.844E+10	4.306E+10	7.812E+18	2.151E+19
13	1.18	12.68	1.612E+10	4.472E+10	8.411E+18	2.317E+19
14	1.04	13.72	1.480E+10	4.146E+10	8.897E+18	2.453E+19
15	1.16	14.88	1.466E+10	5.711E+10	9.433E+18	2.662E+19
16	0.35	15.23	1.341E+10	5.220E+10	9.579E+18	2.719E+19
17	1.45	16.68	1.592E+10	4.815E+10	1.031E+19	2.940E+19

Table 1 cont'd

Calculated Neutron Exposure Rates and Integrated Exposures
at the Surveillance Capsule Center

Iron Atom Displacements

Cycle	Cycle Length [EFPY]	Total Irradiation Time [EFPY]	Displacement Rate [dpa/s]		Displacements [dpa]	
			4 Degrees	40 Degrees	4 Degrees	40 Degrees
1	1.27	1.27	3.381E-11	1.125E-10	1.351E-03	4.494E-03
2	0.78	2.04	3.952E-11	1.411E-10	2.320E-03	7.955E-03
3	0.70	2.75	3.784E-11	1.362E-10	3.162E-03	1.098E-02
4	0.73	3.48	3.658E-11	1.312E-10	4.009E-03	1.402E-02
5	0.74	4.22	3.685E-11	1.368E-10	4.871E-03	1.722E-02
6	0.72	4.95	3.690E-11	1.288E-10	5.712E-03	2.015E-02
7	0.73	5.67	3.707E-11	1.297E-10	6.560E-03	2.313E-02
8	1.12	6.80	3.649E-11	7.225E-11	7.856E-03	2.569E-02
9	1.19	7.98	3.514E-11	7.075E-11	9.174E-03	2.834E-02
10	1.19	9.17	3.119E-11	6.973E-11	1.034E-02	3.096E-02
11	1.14	10.32	3.114E-11	7.075E-11	1.147E-02	3.351E-02
12	1.19	11.51	2.964E-11	7.209E-11	1.258E-02	3.622E-02
13	1.18	12.68	2.591E-11	7.489E-11	1.354E-02	3.900E-02
14	1.04	13.72	2.379E-11	6.939E-11	1.432E-02	4.128E-02
15	1.16	14.88	2.358E-11	9.585E-11	1.519E-02	4.479E-02
16	0.35	15.23	2.157E-11	8.751E-11	1.542E-02	4.574E-02
17	1.45	16.68	2.560E-11	8.076E-11	1.659E-02	4.944E-02

Table 2

Calculated Azimuthal Variation of Maximum Exposure Rates
and Integrated Exposures at the Reactor Vessel
Clad/Base Metal Interface

Cycle	Cycle Length [EFPY]	Total Irradiation Time [EFPY]	Neutron Flux (E > 1.0 MeV) [n/cm^2-s]			
			0 Degrees	15 Degrees	30 Degrees	45 Degrees
1	1.27	1.27	6.258E+09	9.924E+09	1.254E+10	1.901E+10
2	0.78	2.04	7.406E+09	1.195E+10	1.491E+10	2.416E+10
3	0.70	2.75	6.983E+09	1.109E+10	1.413E+10	2.292E+10
4	0.73	3.48	6.755E+09	1.089E+10	1.375E+10	2.212E+10
5	0.74	4.22	6.820E+09	1.090E+10	1.410E+10	2.312E+10
6	0.72	4.95	6.826E+09	1.095E+10	1.366E+10	2.173E+10
7	0.73	5.67	6.856E+09	1.102E+10	1.374E+10	2.188E+10
8	1.12	6.80	6.798E+09	9.609E+09	9.233E+09	1.237E+10
9	1.19	7.98	6.663E+09	8.406E+09	8.819E+09	1.222E+10
10	1.19	9.17	5.725E+09	9.229E+09	9.344E+09	1.182E+10
11	1.14	10.32	5.822E+09	8.829E+09	9.465E+09	1.206E+10
12	1.19	11.51	5.478E+09	8.195E+09	8.953E+09	1.210E+10
13	1.18	12.68	4.791E+09	7.179E+09	9.018E+09	1.256E+10
14	1.04	13.72	4.387E+09	6.675E+09	8.524E+09	1.159E+10
15	1.16	14.88	4.500E+09	7.845E+09	1.074E+10	1.679E+10
16	0.35	15.23	3.985E+09	6.423E+09	9.334E+09	1.480E+10
17	1.45	16.68	4.829E+09	7.703E+09	9.378E+09	1.402E+10

Table 2 cont'd

Calculated Azimuthal Variation of Maximum Exposure Rates
And Integrated Exposures at the Reactor Vessel
Clad/Base Metal Interface

Cycle	Cycle Length [EFPY]	Total Irradiation Time [EFPY]	Neutron Fluence (E > 1.0 MeV) [n/cm^2]			
			0 Degrees	15 Degrees	30 Degrees	45 Degrees
1	1.27	1.27	2.501E+17	3.965E+17	5.009E+17	7.596E+17
2	0.78	2.04	4.299E+17	6.868E+17	8.631E+17	1.346E+18
3	0.70	2.75	5.851E+17	9.333E+17	1.177E+18	1.856E+18
4	0.73	3.48	7.416E+17	1.185E+18	1.496E+18	2.368E+18
5	0.74	4.22	9.011E+17	1.440E+18	1.826E+18	2.909E+18
6	0.72	4.95	1.057E+18	1.690E+18	2.137E+18	3.404E+18
7	0.73	5.67	1.214E+18	1.942E+18	2.451E+18	3.905E+18
8	1.12	6.80	1.455E+18	2.283E+18	2.779E+18	4.343E+18
9	1.19	7.98	1.705E+18	2.598E+18	3.110E+18	4.802E+18
10	1.19	9.17	1.919E+18	2.944E+18	3.460E+18	5.245E+18
11	1.14	10.32	2.129E+18	3.263E+18	3.802E+18	5.680E+18
12	1.19	11.51	2.334E+18	3.569E+18	4.136E+18	6.132E+18
13	1.18	12.68	2.512E+18	3.836E+18	4.471E+18	6.599E+18
14	1.04	13.72	2.656E+18	4.055E+18	4.751E+18	6.980E+18
15	1.16	14.88	2.814E+18	4.330E+18	5.128E+18	7.568E+18
16	0.35	15.23	2.857E+18	4.400E+18	5.229E+18	7.730E+18
17	1.45	16.68	3.071E+18	4.741E+18	5.645E+18	8.351E+18

Note: At the end of Cycle 17, the maximum fast (E > 1.0 MeV) neutron fluences at the pressure vessel wall occur at an axial elevation 15.2 cm above the midplane of the active fuel for the 0°, 15°, 30°, and 45° azimuths.

Table 2 cont'd

Calculated Azimuthal Variation of Fast Neutron Exposure Rates
and Iron Atom Displacement Rates at the Reactor Vessel
Clad/Base Metal Interface

Cycle	Cycle Length [EFPY]	Total Irradiation Time [EFPY]	Iron Atom Displacement Rate [dpa/s]			
			0 Degrees	15 Degrees	30 Degrees	45 Degrees
1	1.27	1.27	1.014E-11	1.588E-11	2.020E-11	3.068E-11
2	0.78	2.04	1.200E-11	1.913E-11	2.406E-11	3.900E-11
3	0.70	2.75	1.131E-11	1.774E-11	2.279E-11	3.699E-11
4	0.73	3.48	1.094E-11	1.742E-11	2.219E-11	3.569E-11
5	0.74	4.22	1.105E-11	1.745E-11	2.275E-11	3.730E-11
6	0.72	4.95	1.106E-11	1.752E-11	2.204E-11	3.508E-11
7	0.73	5.67	1.111E-11	1.763E-11	2.216E-11	3.531E-11
8	1.12	6.80	1.099E-11	1.534E-11	1.487E-11	1.996E-11
9	1.19	7.98	1.076E-11	1.344E-11	1.420E-11	1.972E-11
10	1.19	9.17	9.286E-12	1.474E-11	1.505E-11	1.909E-11
11	1.14	10.32	9.426E-12	1.411E-11	1.523E-11	1.948E-11
12	1.19	11.51	8.848E-12	1.307E-11	1.438E-11	1.948E-11
13	1.18	12.68	7.748E-12	1.147E-11	1.449E-11	2.024E-11
14	1.04	13.72	7.097E-12	1.067E-11	1.369E-11	1.867E-11
15	1.16	14.88	7.290E-12	1.253E-11	1.726E-11	2.701E-11
16	0.35	15.23	6.453E-12	1.027E-11	1.501E-11	2.382E-11
17	1.45	16.68	7.817E-12	1.230E-11	1.508E-11	2.257E-11

Table 2 cont'd

Calculated Azimuthal Variation of Fast Neutron Exposure Rates
and Iron Atom Displacement Rates at the Reactor Vessel
Clad/Base Metal Interface

Cycle	Cycle Length [EFPY]	Total Irradiation Time [EFPY]	Iron Atom Displacements [dpa]			
			0 Degrees	15 Degrees	30 Degrees	45 Degrees
1	1.27	1.27	4.051E-04	6.347E-04	8.073E-04	1.226E-03
2	0.78	2.04	6.964E-04	1.099E-03	1.391E-03	2.173E-03
3	0.70	2.75	9.478E-04	1.494E-03	1.898E-03	2.995E-03
4	0.73	3.48	1.201E-03	1.897E-03	2.412E-03	3.822E-03
5	0.74	4.22	1.460E-03	2.305E-03	2.944E-03	4.694E-03
6	0.72	4.95	1.712E-03	2.704E-03	3.446E-03	5.493E-03
7	0.73	5.67	1.966E-03	3.108E-03	3.954E-03	6.302E-03
8	1.12	6.80	2.356E-03	3.652E-03	4.481E-03	7.010E-03
9	1.19	7.98	2.760E-03	4.156E-03	5.014E-03	7.750E-03
10	1.19	9.17	3.108E-03	4.710E-03	5.578E-03	8.466E-03
11	1.14	10.32	3.448E-03	5.219E-03	6.128E-03	9.169E-03
12	1.19	11.51	3.779E-03	5.707E-03	6.665E-03	9.896E-03
13	1.18	12.68	4.067E-03	6.134E-03	7.204E-03	1.065E-02
14	1.04	13.72	4.300E-03	6.484E-03	7.653E-03	1.126E-02
15	1.16	14.88	4.555E-03	6.924E-03	8.259E-03	1.221E-02
16	0.35	15.23	4.626E-03	7.036E-03	8.422E-03	1.247E-02
17	1.45	16.68	4.973E-03	7.581E-03	9.091E-03	1.347E-02

Note: At the end of Cycle 17, the maximum iron atom displacements at the pressure vessel wall occur at an axial elevation 15.2 cm above the midplane of the active fuel for the 0°, 15°, 30° and 45° azimuths.

Table 3

Relative Radial Distribution Of Neutron Fluence (E > 1.0 MeV)
within the Reactor Vessel Wall

RADIUS (cm)	AZIMUTHAL ANGLE			
	0°	15°	30°	45°
220.35	1.000	1.000	1.000	1.000
225.87	0.544	0.546	0.551	0.540
231.39	0.262	0.263	0.267	0.256
236.90	0.121	0.121	0.124	0.116
242.42	0.056	0.054	0.056	0.049

Note:
Base Metal Inner Radius = 220.35 cm
Base Metal 1/4T = 225.87 cm
Base Metal 1/2T = 231.39 cm
Base Metal 3/4T = 236.90 cm
Base Metal Outer Radius = 242.42 cm

Table 4

Relative Radial Distribution of Iron Atom Displacements (dpa)
within the Reactor Vessel Wall

RADIUS (cm)	AZIMUTHAL ANGLE			
	0°	15°	30°	45°
220.35	1.000	1.000	1.000	1.000
225.87	0.641	0.639	0.652	0.638
231.39	0.395	0.390	0.406	0 387
236.90	0.238	0.235	0.249	0.227
242.42	0.136	0.133	0.142	0.117

Note:
Base Metal Inner Radius = 220 35 cm
Base Metal 1/4T = 225.87 cm
Base Metal 1/2T = 231.39 cm
Base Metal 3/4T = 236.90 cm
Base Metal Outer Radius = 242.42 cm

Table 5

Nuclear Parameters Used in the Evaluation of Neutron Sensors

Monitor Material	Reaction of Interest	Target Atom Fraction	90% Response Range (MeV)	Product Half-life	Fission Yield (%)
Copper	^{63}Cu (n,α)	0.6917	4.9 – 11.8	5.271 y	
Iron	^{54}Fe (n,p)	0.0585	2.1 – 8.3	312.3 d	
Nickel	^{58}Ni (n,p)	0.6808	1.5 – 8.1	70.82 d	
Uranium-238	^{238}U (n,f)	0.9996	1.2 – 6.7	30.07 y	6.02
Neptunium-237	^{237}Np (n,f)	1.0000	0.4 – 3.5	30.07 y	6.17
Cobalt-Aluminum	^{59}Co (n,γ)	0.0015	non-threshold	5.271 y	

Note: The 90% response range is defined such that, in the neutron spectrum characteristic of the D. C. Cook Unit 1 surveillance capsules, approximately 90% of the sensor response is due to neutrons in the energy range specified with approximately 5% of the total response due to neutrons with energies below the lower limit and 5% of the total response due to neutrons with energies above the upper limit.

Table 6

Monthly Thermal Generation during the First Ten Fuel Cycles
of the D. C. Cook Unit 1 Reactor
(Reactor Power of 3250 MWt)

Year	Month	Thermal Generation (MWt-hr)	Year	Month	Thermal Generation (MWt-hr)	Year	Month	Thermal Generation (MWt-hr)
75	1	1,040	78	1	1,923,060	81	1	1,894,240
75	2	18,300	78	2	1,953,625	81	2	2,176,463
75	3	572,000	78	3	2,328,300	81	3	2,411,013
75	4	1,627,271	78	4	438,253	81	4	2,336,161
75	5	1,933,490	78	5	0	81	5	2,254,975
75	6	1,702,931	78	6	230,413	81	6	0
75	7	670,334	78	7	2,256,038	81	7	0
75	8	1,849,116	78	8	2,226,565	81	8	1,790,135
75	9	1,883,324	78	9	2,147,300	81	9	2,333,230
75	10	1,547,637	78	10	2,290,261	81	10	2,411,900
75	11	964,571	78	11	2,306,615	81	11	1,279,657
75	12	1,823,818	78	12	1,681,168	81	12	2,248,410
76	1	1,682,310	79	1	2,299,406	82	1	1,569,517
76	2	1,684,470	79	2	2,091,567	82	2	0
76	3	1,871,720	79	3	2,139,350	82	3	2,024,073
76	4	920,020	79	4	411,763	82	4	2,243,660
76	5	1,099,840	79	5	0	82	5	2,192,908
76	6	2,278,280	79	6	0	82	6	2,329,332
76	7	1,850,650	79	7	762,273	82	7	145,572
76	8	2,400,200	79	8	2,396,428	82	8	0
76	9	1,625,940	79	9	2,313,408	82	9	12,755
76	10	2,417,250	79	10	2,067,631	82	10	1,965,827
76	11	1,913,200	79	11	1,522,934	82	11	2,275,411
76	12	1,740,158	79	12	1,723,754	82	12	2,180,316
77	1	0	80	1	980,650	83	1	2,371,584
77	2	122,284	80	2	2,209,403	83	2	2,154,510
77	3	1,854,264	80	3	2,410,741	83	3	2,215,613
77	4	1,690,059	80	4	2,212,354	83	4	2,298,454
77	5	1,361,490	80	5	2,305,783	83	5	2,075,555
77	6	1,206,310	80	6	0	83	6	2,182,703
77	7	1,553,625	80	7	0	83	7	943,698
77	8	1,746,161	80	8	1,501,561	83	8	0
77	9	1,255,066	80	9	2,100,551	83	9	0
77	10	1,594,097	80	10	2,312,061	83	10	323,110
77	11	1,051,487	80	11	2,293,722	83	11	1,476,269
77	12	2,068,940	80	12	1,833,874	83	12	737,558

Note: Monthly power generation data were obtained from NUREG-0020, "Licensed Operating Reactors Status Summary Report," for the time period spanning January 1975 though March 1989.

Table 6 Cont'd

Monthly Thermal Generation during the First Ten Fuel Cycles
of the D. C. Cook Unit 1 Reactor
(Reactor Power of 3250 MWt)

Year	Month	Thermal Generation (MWt-hr)	Year	Month	Thermal Generation (MWt-hr)
84	1	1,743,010	87	1	2,149,465
84	2	1,940,152	87	2	1,913,061
84	3	2,279,795	87	3	2,099,286
84	4	1,855,391	87	4	969,378
84	5	2,398,744	87	5	2,056,583
84	6	1,861,180	87	6	1,635,814
84	7	2,096,975	87	7	0
84	8	1,349,657	87	8	0
84	9	2,229,693	87	9	0
84	10	2,030,349	87	10	1,326,293
84	11	2,187,769	87	11	2,112,159
84	12	2,115,145	87	12	2,096,851
85	1	699,676	88	1	2,076,972
85	2	2,075,841	88	2	1,997,614
85	3	2,301,237	88	3	2,007,159
85	4	341,767	88	4	2,089,788
85	5	0	88	5	2,156,579
85	6	0	88	6	1,987,237
85	7	0	88	7	2,182,564
85	8	0	88	8	2,300,287
85	9	0	88	9	1,448,245
85	10	0	88	10	1,854,946
85	11	297,751	88	11	1,922,271
85	12	1,109,907	88	12	2,183,754
86	1	2,182,101	89	1	1,846,055
86	2	1,967,273	89	2	1,563,768
86	3	2,180,320	89	3	723,239
86	4	1,901,472			
86	5	2,110,806			
86	6	0			
86	7	819,019			
86	8	1,986,925			
86	9	2,108,718			
86	10	2,181,226			
86	11	2,004,755			
86	12	2,194,212			

Note: Monthly power generation data were obtained from NUREG-0020, "Licensed Operating Reactors Status Summary Report," for the time period spanning January 1975 though March 1989.

Table 7

Calculated $\phi(E > 1.0\ MeV)$ and C_j Factors at the Surveillance Capsule Center
Core Midplane Elevation

Fuel Cycle	$\phi(E > 1.0\ MeV)$ [n/cm^2-s]				C_j			
	Capsule T	Capsule X	Capsule Y	Capsule U	T	X	Y	U
1	6.674E+10	6.674E+10	6.674E+10	6.674E+10	1.000	0.882	0.872	1.052
2		8.360E+10	8.360E+10	8.360E+10		1.105	1.092	1.317
3		8.069E+10	8.069E+10	8.069E+10		1.067	1.054	1.272
4		7.776E+10	7.776E+10	7.776E+10		1.028	1.016	1.225
5			8.106E+10	8.106E+10			1.059	1.277
6			7.634E+10	7.634E+10			0.997	1.203
7				7.689E+10				1.212
8				4.301E+10				0.678
9				4.214E+10				0.664
10				4.151E+10				0.654
Average	6.674E+10	7.564E+10	7.655E+10	6.345E+10	1.000	1.000	1.000	1.000

Table 8

Measured Sensor Activities and Reaction Rates

Surveillance Capsule T

Reaction	Location	Measured Activity (dps/g)	Saturated Activity (dps/g)	Radially Adjusted Saturated Activity (dps/g)	Radially Adjusted Reaction Rate (rps/atom)
$^{63}Cu\ (n,\alpha)\ ^{60}Co$	Top Middle	5.140E+04	3.435E+05	3.280E+05	5.004E-17
	Middle	5.270E+04	3.521E+05	3.363E+05	5.130E-17
	Bottom Middle	6.040E+04	4.036E+05	3.854E+05	5.880E-17
	Average				**5.338E-17**
$^{54}Fe\ (n,p)\ ^{54}Mn$	Top	1.930E+06	3.374E+06	3.543E+06	5.616E-15
	Top Middle	1.690E+06	2.955E+06	3.102E+06	4.918E-15
	Middle	1.690E+06	2.955E+06	3.102E+06	4.918E-15
	Bottom Middle	1.690E+06	2.955E+06	3.102E+06	4.918E-15
	Bottom	1.800E+06	3.147E+06	3.304E+06	5.238E-15
	Average				**5.122E-15**
$^{58}Ni\ (n,p)\ ^{58}Co$	Top Middle	3.830E+07	4.511E+07	5.220E+07	7.473E-15
	Middle	3.770E+07	4.441E+07	5.138E+07	7.356E-15
	Bottom Middle	3.950E+07	4.653E+07	5.383E+07	7.707E-15
	Average				**7.512E-15**
$^{238}U\ (n,f)\ ^{137}Cs$ (Cd)	Middle	1.200E+06	4.190E+07	4.190E+07	2.751E-13
$^{238}U\ (n,f)\ ^{137}Cs$ (Cd)		Including ^{235}U, ^{239}Pu, and γ,fission corrections:			**2.303E-13**
$^{237}Np\ (n,f)\ ^{137}Cs$ (Cd)	Middle	4.530E+06	1.582E+08	1.582E+08	1.009E-12
$^{237}Np\ (n,f)\ ^{137}Cs$ (Cd)			Including γ,fission correction:		**9.935E-13**
$^{59}Co\ (n,\gamma)\ ^{60}Co$	Top	4.870E+09	3.254E+10	3.170E+10	3.102E-12
	Bottom	5.030E+09	3.361E+10	3.274E+10	3.204E-12
	Average				**3.153E-12**
$^{59}Co\ (n,\gamma)\ ^{60}Co$ (Cd)	Top	1.830E+09	1.223E+10	1.409E+10	1.379E-12
	Bottom	1.640E+09	1.096E+10	1.262E+10	1.235E-12
	Average				**1.307E-12**

Note: Measured specific activities are corrected to a shut down date of December 23, 1976.

Table 8 cont'd

Measured Sensor Activities and Reaction Rates

Surveillance Capsule X

Reaction	Location	Measured Activity (dps/g)	Saturated Activity (dps/g)	Radially Adjusted Saturated Activity (dps/g)	Radially Adjusted Reaction Rate (rps/atom)
^{63}Cu (n,α) ^{60}Co	Top Middle	1.140E+05	3.370E+05	3.218E+05	4.910E-17
	Middle	1.150E+05	3.399E+05	3.247E+05	4.953E-17
	Bottom Middle	1.180E+05	3.488E+05	3.331E+05	5.082E-17
	Average				**4.982E-17**
^{54}Fe (n,p) ^{54}Mn	Top	2.210E+06	3.010E+06	3.160E+06	5.010E-15
	Top Middle	2.280E+06	3.105E+06	3.260E+06	5.169E-15
	Middle	2.230E+06	3.037E+06	3.189E+06	5.055E-15
	Bottom Middle	2.340E+06	3.187E+06	3.346E+06	5.305E-15
	Bottom	2.410E+06	3.282E+06	3.446E+06	5.463E-15
	Average				**5.200E-15**
^{58}Ni (n,p) ^{58}Co	Top Middle	3.980E+07	4.471E+07	5.173E+07	7.406E-15
	Middle	4.020E+07	4.516E+07	5.225E+07	7.481E-15
	Bottom Middle	4.180E+07	4.696E+07	5.433E+07	7.778E-15
	Average				**7.555E-15**
^{238}U (n,f) ^{137}Cs (Cd)	Middle	3.640E+05	4.795E+06	4.795E+06	3.148E-14
^{238}U (n,f) ^{137}Cs (Cd)		Including ^{235}U, ^{239}Pu, and γ,fission corrections:			**2.572E-14**
^{237}Np (n,f) ^{137}Cs (Cd)	Middle	2.570E+06	3.385E+07	3.385E+07	2.160E-13
^{237}Np (n,f) ^{137}Cs (Cd)			Including γ,fission correction:		**2.127E-13**
^{59}Co (n,γ) ^{60}Co	Top	1.440E+10	4.257E+10	4.146E+10	4.057E-12
	Bottom	1.400E+10	4.139E+10	4.031E+10	3.945E-12
	Average				**4.001E-12**
^{59}Co (n,γ) ^{60}Co (Cd)	Top	5.520E+09	1.632E+10	1.880E+10	1.840E-12
	Bottom	5.530E+09	1.635E+10	1.883E+10	1.843E-12
	Average				**1.842E-12**

Note. Measured specific activities are corrected to a shut down date of May 30, 1980.

Table 8 cont'd

Measured Sensor Activities and Reaction Rates

Surveillance Capsule Y

Reaction	Location	Measured Activity (dps/g)	Saturated Activity (dps/g)	Radially Adjusted Saturated Activity (dps/g)	Radially Adjusted Reaction Rate (rps/atom)
^{63}Cu (n,α) ^{60}Co	Top Middle	1.470E+05	3.435E+05	3.280E+05	5.004E-17
	Middle	1.480E+05	3.458E+05	3.302E+05	5.038E-17
	Bottom Middle	1.540E+05	3.598E+05	3.436E+05	5.242E-17
	Average				**5.095E-17**
^{54}Fe (n,p) ^{54}Mn	Top	2.320E+06	3.133E+06	3.290E+06	5.215E-15
	Top Middle	2.390E+06	3.228E+06	3.389E+06	5.372E-15
	Middle	2.410E+06	3.255E+06	3.417E+06	5.417E-15
	Bottom Middle	2.460E+06	3.322E+06	3.488E+06	5.529E-15
	Bottom	2.400E+06	3.241E+06	3.403E+06	5.395E-15
	Average				**5.386E-15**
^{58}Ni (n,p) ^{58}Co	Top Middle	3.800E+07	4.654E+07	5.385E+07	7.709E-15
	Middle	3.810E+07	4.666E+07	5.399E+07	7.729E-15
	Bottom Middle	4.030E+07	4.936E+07	5.711E+07	8.175E-15
	Average				**7.871E-15**
^{238}U (n,f) ^{137}Cs (Cd)	Middle	5.260E+05	4.991E+06	4.991E+06	3.277E-14
^{238}U (n,f) ^{137}Cs (Cd)		Including ^{235}U, ^{239}Pu, and γ,fission corrections:			**2.630E-14**
^{237}Np (n,f) ^{137}Cs (Cd)	Middle	3.990E+06	3.786E+07	3.786E+07	2.415E-13
^{237}Np (n,f) ^{137}Cs (Cd)			Including γ,fission correction:		**2.378E-13**
^{59}Co (n,γ) ^{60}Co	Top	1.690E+10	3.949E+10	3.846E+10	3.764E-12
	Bottom	1.660E+10	3.879E+10	3.778E+10	3.697E-12
	Average				**3.731E-12**
^{59}Co (n,γ) ^{60}Co (Cd)	Top	6.800E+09	1.589E+10	1.830E+10	1.791E-12
	Bottom	7.070E+09	1.652E+10	1.903E+10	1.862E-12
	Average				**1.827E-12**

Note: Measured specific activities are corrected to a counting date of July 3, 1982.

Table 8 cont'd

Measured Sensor Activities and Reaction Rates

Surveillance Capsule U

Reaction	Location	Measured Activity (dps/g)	Saturated Activity (dps/g)	Radially Adjusted Saturated Activity (dps/g)	Radially Adjusted Reaction Rate (rps/atom)
^{63}Cu (n,α) ^{60}Co	Top Middle	1.300E+05	2.868E+05	2.739E+05	4.179E-17
	Middle	1.260E+05	2.780E+05	2.655E+05	4.050E-17
	Bottom Middle	1.330E+05	2.935E+05	2.803E+05	4.275E-17
	Average				**4.168E-17**
^{54}Fe (n,p) ^{54}Mn	Top	7.100E+05	2.343E+06	2.460E+06	3.899E-15
	Top Middle	7.340E+05	2.422E+06	2.543E+06	4.031E-15
	Middle	7.310E+05	2.412E+06	2.533E+06	4.015E-15
	Bottom	7.100E+05	2.343E+06	2.460E+06	3.899E-15
	Average				**3.961E-15**
^{58}Ni (n,p) ^{58}Co	Top Middle	2.300E+06	3.543E+07	4.099E+07	5.868E-15
	Middle	2.270E+06	3.497E+07	4.045E+07	5.792E-15
	Bottom Middle	2.360E+06	3.635E+07	4.206E+07	6.021E-15
	Average				**5.894E-15**
^{238}U (n,f) ^{137}Cs (Cd)	Middle	4.490E+05	2.568E+06	2.568E+06	1.686E-14
^{238}U (n,f) ^{137}Cs (Cd)		Including ^{235}U, ^{239}Pu, and γ,fission corrections:			**1.316E-14**
^{237}Np (n,f) ^{137}Cs (Cd)	Middle	2.870E+06	1.641E+07	1.641E+07	1.047E-13
^{237}Np (n,f) ^{137}Cs (Cd)			Including γ,fission correction:		**1.031E-13**
^{59}Co (n,γ) ^{60}Co	Top	2.060E+07	4.545E+07	4.427E+07	2.888E-12
	Bottom	1.930E+07	4.259E+07	4.148E+07	2.706E-12
	Average				**2.797E-12**
^{59}Co (n,γ) ^{60}Co (Cd)	Top	8.660E+06	1.911E+07	2.201E+07	1.436E-12
	Bottom	8.010E+06	1.767E+07	2.036E+07	1.328E-12
	Average				**1.382E-12**

Note: Measured specific activities are indexed to a counting date of October 10, 1989.

Table 9

Comparison of Measured, Calculated, and Best Estimate
Reaction Rates at the Surveillance Capsule Center

Capsule T

	Reaction Rate [rps/atom]				
Reaction	Measured	Calculated	Best Estimate	M/C	M/BE
$^{63}Cu(n,\alpha)^{60}Co$	5.34E-17	4.16E-17	5.14E-17	1.28	1.04
$^{54}Fe(n,p)^{54}Mn$	5.12E-15	4.65E-15	5.33E-15	1.10	0.96
$^{58}Ni(n,p)^{58}Co$	7.51E-15	6.41E-15	7.42E-15	1.17	1.01
$^{59}Co(n,\gamma)^{60}Co$	3.15E-12	2.68E-12	3.13E-12	1.18	1.01
$^{59}Co(n,\gamma)^{60}Co$ (Cd)	1.31E-12	1.40E-12	1.32E-12	0.94	0.99

Capsule X

	Reaction Rate [rps/atom]				
Reaction	Measured	Calculated	Best Estimate	M/C	M/BE
$^{63}Cu(n,\alpha)^{60}Co$	4.98E-17	4.65E-17	4.91E-17	1.07	1.01
$^{54}Fe(n,p)^{54}Mn$	5.20E-15	5.24E-15	5.33E-15	0.99	0.98
$^{58}Ni(n,p)^{58}Co$	7.55E-15	7.23E-15	7.45E-15	1.04	1.01
$^{238}U(n,f)^{137}Cs$ (Cd)	2.57E-14	2.62E-14	2.65E-14	0.98	0.97
$^{237}Np(n,f)^{137}Cs$ (Cd)	2.13E-13	2.06E-13	2.11E-13	1.03	1.01
$^{59}Co(n,\gamma)^{60}Co$	4.00E-12	3.06E-12	3.97E-12	1.31	1.01
$^{59}Co(n,\gamma)^{60}Co$ (Cd)	1.83E-12	1.60E-12	1.83E-12	1.14	1.00

Table 9 cont'd

Comparison of Measured, Calculated, and Best Estimate
Reaction Rates at the Surveillance Capsule Center

Capsule Y

	Reaction Rate [rps/atom]				
Reaction	Measured	Calculated	Best Estimate	M/C	M/BE
$^{63}Cu(n,\alpha)^{60}Co$	5.09E-17	4.70E-17	5.03E-17	1.08	1.01
$^{54}Fe(n,p)^{54}Mn$	5.39E-15	5.30E-15	5.53E-15	1.02	0.97
$^{58}Ni(n,p)^{58}Co$	7.87E-15	7.31E-15	7.73E-15	1.08	1.02
$^{238}U(n,f)^{137}Cs$ (Cd)	2.63E-14	2.65E-14	2.77E-14	0.99	0.95
$^{237}Np(n,f)^{137}Cs$ (Cd)	2.38E-13	2.08E-13	2.28E-13	1.14	1.04
$^{59}Co(n,\gamma)^{60}Co$	3.73E-12	3.10E-12	3.71E-12	1.20	1.01
$^{59}Co(n,\gamma)^{60}Co$ (Cd)	1.83E-12	1.62E-12	1.83E-12	1.13	1.00

Capsule U

	Reaction Rate [rps/atom]				
Reaction	Measured	Calculated	Best Estimate	M/C	M/BE
$^{63}Cu(n,\alpha)^{60}Co$	4.17E-17	3.98E-17	4.04E-17	1.05	1.03
$^{54}Fe(n,p)^{54}Mn$	3.96E-15	4.43E-15	4.16E-15	0.89	0.95
$^{58}Ni(n,p)^{58}Co$	5.89E-15	6.11E-15	5.82E-15	0.96	1.01
$^{59}Co(n,\gamma)^{60}Co$	2.80E-12	2.55E-12	2.79E-12	1.10	1.00
$^{59}Co(n,\gamma)^{60}Co$ (Cd)	1.38E-12	1.33E-12	1.38E-12	1.04	1.00

Table 10

Comparison of Calculated and Best Estimate Exposure Rates
at the Surveillance Capsule Center

Capsule ID	$\phi(E > 1.0\ MeV)$ [n/cm^2-s]			
	Calculated	Best Estimate	Uncertainty (1σ)	BE/C
T	2.667E+18	2.948E+18	7%	1.105
X	8.313E+18	8.440E+18	6%	1.015
Y	1.195E+19	1.258E+19	6%	1.053
U	1.837E+19	1.708E+19	7%	0.930

Capsule ID	Iron Atom Displacement Rate [dpa/s]			
	Calculated	Best Estimate	Uncertainty (1σ)	BE/C
T	4.494E-03	4.863E-03	8%	1.082
X	1.402E-02	1.414E-02	7%	1.009
Y	2.015E-02	2.107E-02	7%	1.046
U	3.096E-02	2.874E-02	9%	0.928

Table 11

Comparison of Measured/Calculated (M/C) Sensor Reaction Rate Ratios including all Fast Neutron Threshold Reactions

Reaction	M/C Ratio			
	Capsule T	Capsule X	Capsule Y	Capsule U
$^{63}Cu(n,\alpha)^{60}Co$	1.28	1.07	1.08	1.05
$^{54}Fe(n,p)^{54}Mn$	1.10	0.99	1.02	0.89
$^{58}Ni(n,p)^{58}Co$	1.17	1.04	1.08	0.96
$^{238}U(n,p)^{137}Cs$ (Cd)	---	0.98	0.99	---
$^{237}Np(n,f)^{137}Cs$ (Cd)	---	1.03	1.14	---
Average	1.19	1.02	1.06	0.97
% Standard Deviation	7.8	3.6	5.6	8.0

Note: The overall average M/C ratio for the set of 16 sensor measurements is 1.06 with an associated standard deviation of 8.7%.

Table 12

Comparison of Best Estimate/Calculated (BE/C) Exposure Rate Ratios

Capsule ID	BE/C Ratio	
	$\phi(E > 1.0$ MeV)	dpa/s
T	1.11	1.08
X	1.02	1.01
Y	1.05	1.05
U	0.93	0.93
Average	1.03	1.02
% Standard Deviation	7.2	6.5

Table 13

Calculated Fast Neutron Exposure of Surveillance Capsules withdrawn from D. C. Cook Unit 1

Capsule	Irradiation Time [EFPY]	Fluence (E > 1.0 MeV) [n/cm^2]	Iron Displacements [dpa]
T	1.27	2.667E+18	4.494E-03
X	3.48	8.313E+18	1.402E-02
Y	4.95	1.195E+19	2.015E-02
U	9.17	1.837E+19	3.096E-02

Table 14

Calculated Maximum Fast Neutron Exposure of the D. C. Cook Unit 1
Reactor Pressure Vessel at the Clad/Base Metal Interface

Neutron Fluence [E > 1.0 MeV]

Cumulative Operating Time [EFPY]	Neutron Fluence [n/cm^2]			
	0.0 Degrees	15.0 Degrees	30.0 Degrees	45.0 Degrees
15.23 (EOC 16)	2.857E+18	4.400E+18	5.229E+18	7.730E+18
16.68 (EOC 17)	3.071E+18	4.741E+18	5.645E+18	8.351E+18
25.00	4.516E+18	7.013E+18	8.397E+18	1.240E+19
32.00	5.745E+18	8.953E+18	1.075E+19	1.587E+19
36.00	6.462E+18	1.008E+19	1.212E+19	1.788E+19
48.00	8.611E+18	1.346E+19	1.621E+19	2.391E+19
54.00	9.686E+18	1.515E+19	1.826E+19	2.692E+19

Iron Atom Displacements

Cumulative Operating Time [EFPY]	Iron Atom Displacements [dpa]			
	0.0 Degrees	15.0 Degrees	30.0 Degrees	45.0 Degrees
15.23 (EOC 16)	4.626E-03	7.036E-038	.422E-031	.247E-02
16.68 (EOC 17)	4.973E-03	7.581E-03	9.091E-03	1.347E-02
25.00	7.317E-03	1.122E-02	1.353E-02	2.002E-02
32.00	9.308E-03	1.432E-02	1.732E-02	2.561E-02
36.00	1.047E-02	1.612E-02	1.952E-02	2.886E-02
48.00	1.396E-02	2.153E-02	2.611E-02	3.860E-02
54.00	1.570E-02	2.423E-02	2.941E-02	4.346E-02

Note: For future projections through 25.00 EFPY, the maximum fast (E > 1.0 MeV) neutron fluences and iron atom displacements at the pressure vessel wall occur at an axial elevation 15.2 cm above the midplane of the active fuel for the 0°, 15°, 30° and 45° azimuths. These peaks at the pressure vessel wall shift such that they occur at an axial elevation of 88.4 cm below the midplane of the active fuel at 36.00 EFPY through 54.00 EFPY for all four azimuthal locations. The future projections also account for a plant uprating from 3250 MWt to 3315 MWt at the onset of cycle 18.

Table 15

Calculated Surveillance Capsule Lead Factors

Cycle	Operating Time [EFPY]	Capsule Lead Factor			
		Capsule T 40°	Capsule X 40°	Capsule Y 40°	Capsule U 40°
1	1.27	3.51	3.51	3.51	3.51
2	2.04		3.51	3.51	3.51
3	2.75		3.51	3.51	3.51
4	3.48		3.51	3.51	3.51
5	4.22			3.51	3.51
6	4.95			3.51	3.51
7	5.67				3.51
8	6.80				3.51
9	7.98				3.50
10	9.17				3.50

Cycle	Operating Time [EFPY]	Capsule Lead Factor			
		Capsule W[1] 4°/40°	Capsule V 4°	Capsule S[1] 4°	Capsule Z 4°
1	1.27	1.10	1.10	1.10	1.10
2	2.04	1.07	1.07	1.07	1.07
3	2.75	1.06	1.06	1.06	1.06
4	3.48	1.05	1.05	1.05	1.05
5	4.22	1.04	1.04	1.04	1.04
6	4.95	1.04	1.04	1.04	1.04
7	5.67	1.04	1.04	1.04	1.04
8	6.80	1.12	1.12	1.12	1.12
9	7.98	1.19	1.19	1.19	1.19
10	9.17	1.22	1.22	1.22	1.22
11	10.32	1.25	1.25	1.25	1.25
12	11.51	1.27	1.27	1.27	1.27
13	12.68	1.27	1.27	1.27	1.27
14	13.72	1.27	1.27	1.27	1.27
15	14.88	1.45	1.25	1.25	1.25
16	15.23	1.49	1.24	1.24	1.24
17	16.68	1.65	1.23	1.23	1.23
	25.00	2.24	1.22	1.22	1.22
	32.00	2.49	1.21	1.21	1.21
	36.00	2.59	1.20	1.20	1.20
	48.00	2.78	1.19	1.19	1.19
	54.00	2.84	1.18	1.18	1.18

Note:

1. Capsule W was formally located at the 4° position and known as Capsule S. Capsule S was formally known as Capsule W. These changes are documented in Reference 4.

References

1. Regulatory Guide 1.190, "Calculational and Dosimetry Methods for Determining Pressure Vessel Neutron Fluence," U. S. Nuclear Regulatory Commission, Office of Nuclear Regulatory Research, March 2001.
2. WCAP-14040-NP-A, Revision 2, "Methodology Used to Develop Cold Overpressure Mitigating System Setpoints and RCS Heatup and Cooldown Limit Curves," January 1996.
3. WCAP-15557, Revision 0, "Qualification of the Westinghouse Pressure Vessel Neutron Fluence Evaluation Methodology," August 2000.
4. AEP Safety Review Screening Checklist CE-95-0309, September 1995.
5. NTSD/SI-598/88, "Cook Rerating, AEPSC Input," February 1988.
6. WCAP-12483, "Analysis of Capsule U from the American Electric Power Company D. C. Cook Unit 1 Reactor Vessel Radiation Surveillance Program," January 1990.
7. WCAP-10376, "Core Physics Characteristics of the Donald C. Cook Station Nuclear Plant (Unit 1, Cycle 8)," July 1983.
8. WCAP-10862, "Core Physics Characteristics of the Donald C. Cook Station Nuclear Plant (Unit 1, Cycle 9)," August 1985.
9. WCAP-11586, "Nuclear Parameters and Operations Package for the Donald C. Cook Station Nuclear Plant (Unit 1, Cycle 10)," October 1987.
10. WCAP-12153, "Nuclear Parameters and Operations Package for the Donald C. Cook Station Nuclear Plant (Unit 1, Cycle 11)," June 1989.
11. WCAP-12797, "Nuclear Parameters and Operations Package for the Donald C. Cook Nuclear Plant (Unit 1, Cycle 12)," December 1990.
12. WCAP-13482, "Nuclear Parameters and Operations Package for the Donald C. Cook Nuclear Plant (Unit 1, Cycle 13)," August 1992.
13. WCAP-13955, "Nuclear Parameters and Operations Package for the Donald C. Cook Nuclear Plant (Unit 1, Cycle 14)," April 1994.
14. WCAP-14465, Revision 1, "Nuclear Parameters and Operations Package for the Donald C. Cook Nuclear Plant (Unit 1, Cycle 15)," October 1995.
15. WCAP-14852, "Nuclear Parameters and Operations Package for the Donald C. Cook Nuclear Plant (Unit 1, Cycle 16)," March 1997.
16. WCAP-15594, "Nuclear Parameters and Operations Package for the Donald C. Cook Nuclear Plant (Unit 1, Cycle 17)," October 2000.
17. RSICC Computer Code Collection CCC-650, "DOORS 3.1, One, Two- and Three Dimensional Discrete Ordinates Neutron/Photon Transport Code System," August 1996.
18. RSIC Data Library Collection DLC-185, "BUGLE-96, Coupled 47 Neutron, 20 Gamma-Ray Group Cross Section Library Derived from ENDF/B-VI for LWR Shielding and Pressure Vessel Dosimetry Applications," March 1996.
19. A. Schmittroth, *FERRET Data Analysis Core*, HEDL-TME 79-40, Hanford Engineering Development Laboratory, Richland, WA, September 1979.
20. RSIC Data Library Collection DLC-178, "SNLRML Recommended Dosimetry Cross-Section Compendium", July 1994

APPENDIX A

RADIAL POWER DISTRIBUTIONS USED IN THE TRANSPORT CALCULATIONS FOR D. C. COOK UNIT 1

Average Radial Core Power Distribution
Cycle 1

Relative Power

1.141	1.152	1.151	1.164	1.164	1.186	1.022	0.743
1.154	1.139	1.094	1.148	1.159	1.125	1.009	0.796
1.152	1.099	1.129	1.142	1.134	1.145	0.962	0.682
1.167	1.149	1.143	1.133	1.070	1.067	0.979	0.589
1.170	1.160	1.135	1.070	1.204	0.942	0.854	
1.162	1.120	1.146	1.062	0.941	0.997	0.513	
1.017	1.006	0.964	0.974	0.842	0.511		
0.743	0.792	0.681	0 586				

Average Radial Core Power Distribution
Cycle 2

Relative Power

1.106	0.823	0.902	0 847	0.872	1.127	1.055	0.973
0.820	0.867	1.094	0.996	0.897	1.121	1.244	0.994
0.902	1.095	0.877	0.895	1.076	0.984	1.203	0.952
0.857	0.999	0.895	0.877	1.044	1.030	1.171	0.736
0.861	0.897	1.074	1.040	1.058	1.104	1.017	
1.097	1.112	0.992	1.041	1.106	1.184	0.737	
1.025	1.234	1.192	1.161	1.008	0.740		
0.970	0.979	0.951	0.733				

Average Radial Core Power Distribution
Cycle 3

Relative Power

0.951	0.894	1.075	0.939	1.100	0.870	0.930	0.907
0.901	0.940	1.158	1.163	1.108	0.893	1.224	0.922
1.089	1.160	0.950	1.172	1.171	1.076	0.913	0.853
0.947	1.169	1 168	0.971	1.168	0.971	1.157	0.675
1.095	1.109	1.170	1.163	0.955	0.964	0 963	
0.848	0.886	1.078	0.965	0.964	1.110	0.683	
0.904	1.205	0.912	1.138	0.952	0.684		
0 897	0.916	0.847	0.668				

Average Radial Core Power Distribution
Cycle 4

Relative Power

0.929	1.077	0.985	1.057	1.061	0.823	0.908	0.870
1.091	0.978	1.152	1.014	1.143	0.951	1.144	0.908
0.991	1.131	1.016	1.187	1.147	1.120	0.923	0.833
1.066	1.024	1.185	1.016	1.151	1.010	1.118	0.660
1.060	1.129	1.146	1.146	1.089	0.966	0.926	
0.855	0.950	1.115	0.999	0.973	1.082	0.678	
0.922	1.169	0.927	1.103	0.914	0.667		
0.875	0.894	0.835	0.679				

Average Radial Core Power Distribution
Cycle 5

Relative Power

1.103	0.848	0.951	1.093	0.974	0.860	0.941	0.877
0.853	0.915	1.117	1.027	1.121	0.920	1.176	0.898
0.955	1.117	1.018	1.199	1.119	1.094	0.937	0.824
1.096	1.009	1.197	1.190	1.178	0.986	1.129	0.657
0.964	1.128	1.118	1.178	0.977	1.069	0.955	
0.841	0.918	1.104	0.997	1.066	1.135	0.692	
0.945	1.187	0.944	1.117	0.945	0.690		
0.877	0.896	0.825	0.668				

Average Radial Core Power Distribution
Cycle 6

Relative Power

1.019	1.027	1.007	1.149	0.978	0.898	0.917	0.879
1.028	0.925	1.147	1.136	1.140	0.938	1.187	0.909
1.002	1.148	0.959	1.135	1.167	1.067	0 950	0.843
1.147	1.139	1.138	1.006	1.172	1.003	1.143	0.669
0.980	1.140	1.170	1.173	0.938	0.950	0.910	
0.876	0.940	1.067	1.002	0.949	1.055	0.658	
0.917	1.193	0.951	1.143	0.911	0.656		
0 879	0.908	0.844	0.673				

Average Radial Core Power Distribution
Cycle 7

Relative Power

0.883	1.043	0.962	1.130	0.920	0.871	0.923	0.891
1.041	0.996	1.156	1.107	1.115	0.917	1.190	0.909
0.963	1.153	0.988	1.114	1.176	1.119	0.952	0.853
1.130	1.108	1.114	0.996	1.185	0.993	1.149	0.679
0.919	1.116	1.181	1.189	0.978	0.945	0.912	
0.857	0.917	1.121	0.993	0.944	1.057	0.663	
0.925	1.191	0.951	1.150	0.912	0.663		
0.891	0.909	0.853	0.680				

Average Radial Core Power Distribution
Cycle 8

0.842	1.027	0.938	1.091	1.142	1.212	0.995	0.957
1.027	1.072	1.193	0.995	1.218	1.008	1.218	0.931
0.938	1.193	1.008	1.186	1.110	1.250	1.129	0.880
1.091	0.995	1.186	0.969	1.148	1.110	1.040	0.421
1.142	1.218	1.110	1.148	1.084	1.110	0.631	
1.212	1.008	1.250	1.110	1.110	0 753	0.319	
0.995	1.218	1.129	1.040	0.631	0.319		
0.957	0.931	0.880	0.421				

Average Radial Core Power Distribution
Cycle 9

Relative Power

1.022	1.101	1.071	1.237	0.949	1.111	1.109	0.931
1.111	1.163	1.263	0 996	1.248	1.075	1.258	0.920
1.079	1.268	1.006	1.274	1.095	1.278	1.052	0.670
1.265	0.993	1.281	1.027	1.270	1.031	1.049	0.419
1.086	1.282	1.101	1.271	0.921	1.094	0.580	
1.141	1.085	1.263	1.025	1.125	0.726	0.281	
1.116	1.241	0.946	1.012	0.627	0.293		
0.923	0.898	0.625	0.344				

Average Radial Core Power Distribution
Cycle 10

Relative Power

0.980	1.041	1.019	0.993	1.036	1.028	0.971	0.641
1.041	1.068	1.240	1.042	1.271	1.161	1.244	0.881
1.013	1.235	1.058	1.262	1.127	1.288	1.106	0.792
0.994	1.045	1.259	1.035	1.267	1.059	1.079	0.396
1.031	1.270	1.121	1.269	1.091	1.124	0.617	
1.020	1.164	1.292	1.066	1.134	0.577	0 243	
0.949	1.232	1.115	1.096	0.630	0.304		
0.540	0.854	0.796	0.436				

Average Radial Core Power Distribution
Cycle 11

Relative Power

0.906	1.236	0.963	1.272	1.101	1.266	0.961	0.775
1.236	1.081	1.236	1.078	1.267	0.948	1.186	0.659
0.964	1.236	1.057	1.115	1.091	1.251	1.053	0.764
1.271	1.078	1.117	1.085	1.284	1.157	1.063	0.415
1.097	1.264	1.090	1.286	1.095	1.173	0.694	
1.259	0.942	1.249	1.160	1.175	0.652	0.289	
0.975	1.190	1.049	1.063	0.699	0.290		
0.814	0.669	0.764	0.411				

Average Radial Core Power Distribution
Cycle 12

Relative Power

0.999	1.262	1.013	1.260	1.006	1.259	1.173	0.903
1.259	1.005	1.051	1.063	1.257	0 955	1.228	0.718
1.008	1.047	1.021	1.254	1.087	1.249	0.996	0.793
1.241	1.054	1.254	0.961	1.260	1.057	1.072	0.446
0.945	1.247	1.086	1.263	1.046	1.174	0.730	
1.254	0.950	1.248	1.058	1.178	0.749	0.309	
1.164	1.224	0.994	1.073	0.735	0.333		
0.899	0.715	0.792	0.446				

Average Radial Core Power Distribution
Cycle 13

Relative Power

0.919	1.301	1.047	1.120	1.063	1.003	1.267	0.614
1.304	0.967	1.230	1.085	1.230	1.023	1.197	0.691
1.050	1.233	0.970	1.253	1.045	1.071	1.234	0.557
1.121	1.086	1.253	1.087	1.265	1.093	1.127	0 385
1.065	1.231	1.042	1.265	1.072	1.234	0.827	
1.008	1.024	1.070	1.094	1.234	0.725	0.334	
1.269	1.198	1.234	1.127	0.829	0.340		
0.616	0.691	0.557	0.385				

Average Radial Core Power Distribution
Cycle 14

Relative Power

0.918	1.293	1.018	1.064	1.099	1.084	1.260	0.573
1.296	0.968	1.257	1.047	1.271	1.054	1.193	0.614
1.022	1.260	1.067	1.286	1.150	1.124	1.212	0.514
1.064	1.047	1.284	1.001	1.298	1.042	1.101	0.337
1.099	1.270	1.148	1.296	1.132	1.223	0.814	
1.084	1.055	1.125	1.044	1.224	0.695	0.318	
1.261	1.195	1.220	1.113	0 817	0.308		
0.574	0.616	0.521	0.364				

Average Radial Core Power Distribution
Cycle 15

Relative Power

0.869	1.230	0.922	1.274	0.917	1.087	1.186	0.578
1.232	0.895	1.195	1.046	1.281	1.111	1.258	0.585
0.922	1.195	0.932	1.269	0 892	1.027	1.250	0.604
1.275	1.045	1.267	0.988	1.012	1.244	1.156	0.410
0.917	1.281	0.892	1.012	1.244	1.105	0.878	
1.092	1.111	1.025	1.248	1.104	1.058	0.505	
1.177	1.256	1.262	1.175	0.877	0.485		
0.535	0.581	0 618	0.482				

Average Radial Core Power Distribution
Cycle 16

Relative Power

0.688	0.916	0.970	1.252	1.125	1.120	1.225	0.504
0.909	1.010	1.209	1.039	1.274	1.097	1.218	0.498
0.966	1.208	1.029	1.277	1.120	1.070	1.189	0.513
1.232	1.037	1.279	1.084	1.296	1.089	1.105	0.335
1.122	1.269	1.120	1.301	1.155	1.225	0.887	
1.110	1.091	1.068	1.089	1.225	1.057	0.397	
1.219	1.214	1.186	1.104	0.887	0.397		
0.503	0.496	0.511	0.335				

Average Radial Core Power Distribution
Cycle 17

Relative Power

0.956	1.162	0.934	1.178	1.223	1.173	1.190	0.577
1.161	0.983	1.278	0.954	0.969	0.975	1.198	0.724
0.933	1.276	0.988	1.177	1.218	1.178	1.251	0 691
1.177	0.954	1.176	1.288	1.016	1.187	1.044	0 411
1.222	0 967	1.214	1.013	1.258	1.097	0.819	
1.172	0.974	1.175	1.181	1.088	0.939	0 401	
1.190	1.197	1.248	1.034	0.816	0.400		
0.577	0.723	0.690	0.409				

ATTACHMENT 5 TO AEP:NRC:2900-02

APPLICABILITY OF NRC QUESTIONS PERTAINING TO UNIT 2 REACTOR COOLANT SYSTEM PRESSURE-TEMPERATURE CURVE CHANGES

In a letter dated July 23, 2002 (Reference 1), Indiana Michigan Power Company (I&M) proposed to revise the Unit 2 RCS pressure-temperature curves. By Reference 2, the NRC requested additional information regarding the amendment proposed by Reference 1. Although the Unit 2 licensing activity proposed by Reference 1 is unrelated to the proposed Unit 1 RCS pressure-temperature curve applicability limit changes, I&M has reviewed the NRC's questions for impact on the changes proposed by this letter. This attachment presents I&M's responses to the NRC's questions, as applied to the proposed Unit 1 pressure-temperature curve applicability limit changes.

NRC Question 1

What is the physical basis for the calculated peak inside surface E > 1.0 MeV at 32 effective full power years to be lower than the original FERRET Code adjusted value? This plant has a thermal shield and the transport cross sections were changed to ENDF/B-VI which should have increased the original value.

Response to Question 1

This question is not applicable to the Donald C. Cook Nuclear Plant (CNP) Unit 1 measurement uncertainty recapture (MUR) uprate, since the end-of-life (EOL) (i.e., 32 effective full power years (EFPY)) peak fluence value that is currently being used for the Unit 1 Reactor Coolant System (RCS) pressure-temperature curves is less than the EOL peak fluence under the MUR uprate conditions. Specifically, the peak fluence at 32 EFPY identified in Table 14 of Attachment 4 to this letter is 1.587×10^{19} neutrons per square centimeter (n/cm^2), which is higher than the previous capsule report (WCAP-12483, Rev. 0, as submitted by Reference 6) value of 1.41×10^{19} n/cm^2.

NRC Question 2

Is the old and the new FERRET Code the same? (We noted that the calculated value was used and not the FERRET Code adjusted value).

Response to Question 2

The FERRET code is a linear least squares adjustment code. The FERRET code itself has not been changed between the Capsule U application documented in Reference 6 and the current application documented in Attachment 4 to this letter. However, due to the evolution from

ENDF/B-IV to ENDF/B-VI cross-sections, some of the inputs to the adjustment procedure have changed.

There are three fundamental inputs to the FERRET adjustment procedure. These are:

1. The calculated neutron energy spectrum and associated uncertainties.

2. The dosimetry reaction cross-sections and associated uncertainties.

3. The measured dosimeter reaction rates and associated uncertainties.

In current evaluations, the calculated neutron energy spectra are based on discrete ordinates transport calculations using ENDF/B-VI cross-sections and the uncertainties are based on the latest benchmarking comparisons and sensitivity studies. Prior evaluations used calculations based on ENDF/B-IV transport cross-sections. The ENDF/B-VI analyses result in an increase in the magnitude of the calculated spectra and a reduction in the uncertainty associated with the calculations.

The dosimetry reaction cross-sections used in the current least squares analyses are, likewise, based on the latest ENDF/B-VI data and include extensive uncertainty evaluations. The dosimetry cross-section data set used by Westinghouse is recommended by the American Society for Testing and Materials (ASTM) for light water reactor applications (ASTM E1018-01, "Standard Guide for Application of ASTM Evaluated Cross Section Data File, Matrix E 706 (IIB)," 2002). Prior least squares evaluations used dosimetry cross-sections obtained from the ENDF/B-IV and ENDF/B-V data files.

Measured reaction rates have not changed in the CNP Unit 1 analyses.

NRC Question 3

The former plates have been added to the revised analysis. Were any of the dosimeters in the shadow of the former plates? Is the peak location in the shadow of the former plates?

Response to Question 3

Based on the following discussion, it is shown that four dosimetry sets (top-middle, middle, bottom-middle, and bottom) are in the shadow of the former plates. However, the peak location; i.e., maximum pressure vessel fluence, is not in the shadow of the former plates.

Considering the midplane of the active fuel as Z = 0.0, the elevation of the former plates relative to the core midplane is summarized as follows:

Component	Height [cm]
Core Top	182.88
Former 7	140.90 to 144.39
Former 6	89.69 to 93.19
Former 5	38.49 to 41.98
Core Midplane	0.00
Former 4	-16.38 to –12.88
Former 3	-67.58 to –64.09
Former 2	-118.79 to –115.30
Former 1	-173.65 to –170.16
Core Bottom	-182.88

Relative to the maximum pressure vessel fluences listed in Table 14 of Attachment 4 to this letter, the fluence values given for 25 EFPY of operation occur at an elevation of approximately +15 centimeters (cm); i.e., 15 cm above core midplane. Due to the average axial shape used in the future fluence projections for 32, 36, 48, and 54 EFPY, the location of the maximum pressure vessel fluence shifts to an elevation of approximately -88 cm; i.e., 88 cm below core midplane. Both of these axial elevations are located midway between former plates. Therefore, the peak location is not in the shadow of the former plates.

The surveillance capsules incorporated into the CNP Unit 1 reactor are centered on the core midplane (Z = 0.0) and have a specimen stack height of 99.56 cm. Thus, the capsules span an axial range extending from –49.78 to +49.78 cm relative to the core midplane. From the table above, it can be seen that only formers 4 and 5 impact this axial span. Former 4 is located below the midplane of the specimen stack and former 5 is positioned near the top of the stack.

Dosimeters are located within the specimen stack at five axial elevations designated top, top-middle, middle, bottom-middle, and bottom. The following tabulation indicates the axial center of the specimens containing dosimeter wires.

Dosimeter Designation	Center of Dosimetry Set [cm]
Top	44.38
Top-Middle	18.85
Middle	-1.97
Bottom-Middle	-25.49
Bottom	-47.08

From this tabulation, it is noted that the neutron sensors positioned at the top-middle, middle, bottom-middle, and bottom axial elevations are located well away from the formers. The sensors located at the top elevation are positioned near the axial location of former 5.

In each capsule, the positioning of former 5 has the potential to impact the measurements obtained with one iron wire, one bare cobalt-aluminum wire, and one cadmium-covered cobalt-aluminum wire. Of these, only the iron wire has an impact on fast neutron evaluations. In the CNP Unit 1 application, iron wires are placed at all five axial elevations. An examination of Table 8 of Attachment 4 shows that for all four capsules removed from Unit 1 there is no statistically significant difference between iron measurements at the top location and measurements obtained at the other four axial locations. It can be concluded, therefore, that the presence of former 5 has a minimal impact on the measurements obtained near the top of the capsule.

NRC Question 4

The γ-fission, U-235 impurity, and Pu-239 built-in corrections (Page 6-8) seem to be new in the revision. How were these corrections derived?
[I&M Note: This question refers to Page 6-8 of WCAP-13515 (Attachment 3 to Reference 1).]

Response to Question 4

The γ fission corrections to the U-238 and Np-237 fission dosimeters are now standard practice for dosimetry evaluations, in accordance with Regulatory Guide 1.190, Regulatory Position 2.1.2. The corrections were determined for each capsule location from the results of the ENDF/B-VI transport calculations using the BUGLE-96 library. The transport calculations were completed for the entire 67 group structure (47 neutron, 20 gamma ray) included in the BUGLE-96 library. From these calculations, the ratio of gamma ray-induced fission to neutron-induced fission was obtained for both of the fission sensors. Based on these calculated ratios, the correction factors associated with the Unit 1 capsules were determined as follows.

Capsule ID and Location	**Ratio [U-238(γ,f)]/[U-238(n,f)]**	**(γ,f) Correction $[1+Ratio]^{-1}$**
T (40 Degrees)	0.0439	0.958
X (40 Degrees)	0.0439	0.958
Y (40 Degrees)	0.0439	0.958
U (40 Degrees)	0.0439	0.958

Capsule ID and Location	Ratio [Np-237(γ,f)]/[Np-237(n,f)]	(γ,f) Correction $[1+Ratio]^{-1}$
T (40 Degrees)	0.0156	0.985
X (40 Degrees)	0.0156	0.985
Y (40 Degrees)	0.0156	0.985
U (40 Degrees)	0.0156	0.985

The data in the above tables indicates that the gamma ray-induced fission corrections for the Unit 1 fission sensors are approximately 4 percent and 1.5 percent for U-238 and Np-237, respectively.

Additional corrections for trace impurities of U-235 and for the build-in of plutonium isotopes in U-238 fission sensors have always been a part of dosimetry evaluations performed by Westinghouse. Due to the conversion of U-238 to Pu-239 over time, these corrections are a function of the total fluence accrued by the individual sensors. That is, the longer the irradiation the greater the impact of plutonium fissioning. The corrections used in the CNP Unit 1 dosimetry evaluations were obtained using the ORIGEN code to develop a correlation defining the U-238(n,f) contribution to the total integrated fissions in the dosimeter as a function of the neutron fluence experienced by the sensor. The specific corrections used in the evaluation of the Unit 1 U-238 sensors are summarized as follows:

Capsule ID and Location	Calculated Fluence (E > 1.0 MeV) [n/cm^2]	Fractional U-238 Contribution
T (40 Degrees)	2.667e+18	0.874
X (40 Degrees)	8.313e+18	0.853
Y (40 Degrees)	1.195e+19	0.838
U (40 Degrees)	1.837e+19	0.815

NRC Question 5

It is stated that a 10 percent positive bias was applied to the neutron sources for Cycles 13 and on. Was there also an assumption of low leakage loadings made for the same cycles?

Response to Question 5

This question is not applicable to the fluence evaluation supporting the Unit 1 MUR uprate, as a bias factor on the periphery was not used. This question will be applicable for the letter that will submit the new Unit 1 pressure-temperature curves, as the new pressure-temperature curves will be based on an evaluation that did include a 10 percent positive bias on the periphery.

REFERENCES

1. Letter from J. E. Pollock, I&M, to NRC Document Control Desk, "License Amendment Request for Unit 2 Reactor Coolant System Pressure-Temperature Curves, and Request for Exemption from Requirements in 10 CFR 50.60(a) and 10 CFR 50, Appendix G," AEP:NRC:2349-01, dated July 23, 2002
2. Letter from J. F. Stang, NRC, to A. C. Bakken III, I&M, "Donald C. Cook Nuclear Plant, Unit 2 – Request for Additional Information Regarding License Amendment Request, 'Reactor Coolant System Pressure – Temperature Curves,' dated July 23, 2002," dated September 27, 2002
3. WCAP-13515, Rev. 1, "Analysis of Capsule U from the Indiana Michigan Power Company D. C. Cook Unit 2 Reactor Vessel Radiation Surveillance Program," May 2002 (Attachment 3 to AEP:NRC:2349-01)
4. WCAP-15047, Rev. 2, "D. C. Cook Unit 2 WOG Reactor Vessel 60-Year Evaluation Minigroup Heatup and Cooldown Limit Curves for Normal Operation," May 2002 (Attachment 4 to AEP:NRC:2349-01)
5. WCAP-13517, Rev. 1, "Evaluation of Pressurized Thermal Shock for D. C. Cook Unit 2," May 2002 (Attachment 5 to AEP:NRC:2349-01)
6. Letter from M. P. Alexich, I&M, to T. E. Murley, NRC, "Reactor Vessel Material Surveillance Reports," correspondence number AEP:NRC:0894M, dated June 22, 1990

ATTACHMENT 6 TO AEP:NRC:2900-02

REGULATORY COMMITMENTS

The following table identifies those actions committed to by Indiana Michigan Power Company (I&M) in this document. Any other actions discussed in this submittal represent intended or planned actions by I&M. They are described to the Nuclear Regulatory Commission (NRC) for the NRC's information and are not regulatory commitments.

Commitment	Date
I&M will submit a proposed license amendment containing new Unit 1 RCS pressure-temperature curves that reflect the limiting reactor vessel beltline material. I&M does not intend to include new low temperature overpressure protection setpoints in the proposed amendment unless the new pressure-temperature curves are more restrictive than the existing curves. This commitment supercedes I&M's previous commitment, made in Reference 4, to submit revised curves by April 30, 2004.	December 31, 2002